PERGAMON

Quaternary Science Reviews 22 (2003) 2285–2302

QSR

Late Weichselian (Valdaian) and Holocene vegetation and environmental history of the northern Timan Ridge, European Arctic Russia

Aage Paus[a,*], John Inge Svendsen[b], Alexei Matiouchkov[c]

[a] *Department of Botany, University of Bergen, N-5007 Bergen, Norway*
[b] *Department of Earth Science, University of Bergen, Allégt. 41, N-5007 Bergen, Norway*
[c] *VSEGEI (National Geological Institute), Sredny pr.74, St. Petersburg 199126, Russia*

Received 10 July 2002; accepted 18 April 2003

Abstract

Lake and peat deposits from the Timan Ridge, Arctic Russia, were pollen analysed, reconstructing the vegetation history and paleoenvironment since the Last Glacial Maximum (LGM) 20–18,000 years ago. The sites studied are located inside the margins of a large paleolake of about 20 km^2, by us named Lake Timan. This lake developed in the Late Weichselian, more than 30,000 years after the deglaciation of this region, and was formed due to increased precipitation and warmer summers that accelerated the melting of stagnant ice within its catchment. The lake was drained during the early Holocene when the outlet rivers eroded the spillways. A new generation of much smaller lakes formed during the Holocene when the last remnants of buried glacier ice melted away causing the exposed floor of Lake Timan to subside. Since deglaciation, the following regional vegetation development has been recorded: (1) During the initial stage of Lake Timan, the dominant vegetation was discontinuous steppe/tundra, with patches of snow bed vegetation. (2) A dwarf-shrub tundra established during the Late Weichselian interstadial (Allerød), probably reflecting warmer and moister conditions. (3) The Younger Dryas cooling is recognised by a reversal to steppe/tundra and snowbeds on unstable mineral-soils, and higher palynological richness. (4) Soon after the transition into the Holocene, a birch-forest established on the Timan Ridge. (5) A cooling starting around 8200 cal. years BP initiated the deforestation of the exposed hills. In the most protected sites, birch trees persisted until later than 4000 years ago, reflecting a gradual development into the present treeless dwarf-shrub tundra.
© 2003 Elsevier Science Ltd. All rights reserved.

1. Introduction

The paleoenvironment and vegetation history in northern European Russia is poorly known (see Khotinsky, 1984; Peterson, 1993). Holocene studies exist from east of the Pechora river (e.g. Davydova and Servant-Vildary, 1996; Kaakinen and Eronen, 2000) and from Kola and Karelia in the west (e.g. Elina and Kuznetskov, 1996; Kremenetski and Patyk-Kara, 1997; Kremenetski et al., 1997; Velichko et al., 1997; Jankovska et al., 1999; Snyder et al., 2000). Here we present the results of geological and pollen-analytical studies from the Timan Ridge close to the Barents Sea coast in the European part of the Russian Arctic. In this area, sediments of a Late Weichselian paleolake and the exposed layers of a Holocene peat bog were studied. This area is ecotonally positioned just north of the present subarctic tree-birch vegetation. Detailed paleobotanical analyses have provided a continuous record of the environmental development from near the Last Glacial Maximum (LGM, 20–18 ka) and up to the present. The pollen stratigraphy reveal significant displacements of vegetation belts through time.

2. Study area and sample sites

2.1. Geology and glacial history

The Timan Ridge is a low north-south trending bedrock ridge forming a barrier between the Pechora

*Corresponding author. Tel.: +47–55-58-33-44.
E-mail address: aage.paus@bot.uib.no (A. Paus).

0277-3791/03/$ - see front matter © 2003 Elsevier Science Ltd. All rights reserved.
doi:10.1016/S0277-3791(03)00136-7

Lowland and the White Sea Basin. Our study area (67°16′N, 48°43′E) is located in the northern part of the ridge, ca 30 km south of the Barents Sea coast. This is 5–10 km inside the Markhida-Pyoza moraines deposited by the Barents–Kara Ice Sheet during the early Middle Weichselian some 60–50 ka (Fig. 1) (cf. Astakhov et al., 1999; Mangerud et al., 1999). At the LGM, the Barents–Kara Ice Sheet terminated on the continental shelf in the Pechora Sea north of the Timan Ridge, whereas the margin of the Scandinavian Ice Sheet was located in the Mezen drainage basin about 200 km further west (Svendsen et al., 1999, Svendsen et al. submitted). The landscape, slightly undulating between 150 and 200 m a.s.l., is covered by a veneer of Quaternary sediments with visible bedrock at the highest altitudes. Bedrock is metamorphic Precambrian bedrock (Khain, 1985), and Quaternary deposits consist of glacial deposits including tills and glaciofluvial and lacustrine sediments (Lavrov et al., 1991). Geomorphologically, the study area is characterised by some conspicuous north-south trending esker ridges and many fresh looking kettle holes (Figs. 1 and 2). A horizontal break of slope at about 170–180 m a.s.l. is distinct in several slopes and was traced in some areas for several kilometres on air photographs (Figs. 1 and 2). In field, these lines appeared as erosional features that we interpret as a system of shorelines incised into the glacial deposits. According to our mapping, they outline the existence of a more than 20 km^2 large paleolake (Mangerud et al., 1999) that we have named Lake Timan. This interpretation is substantiated by: (1) Within the margins of the of Lake Timan, the terrain is smoothed and partly draped by silt/clay. Outside, a hummocky glacial landscape (Fig. 2) is without any traces of flooding. (2) Fossil ice wedge polygons are frequent above the inferred shorelines but almost absent below. (3) The highest shorelines, up to 20–30 m above the present local lakes, imply that Lake Timan had outlets at the same level. At several places, esker ridges that according to our mapping once dammed the lake, are cut through by narrow erosional gaps (Figs. 1 and 2). These point to a superimposed fluvial incision reflecting a falling water level.

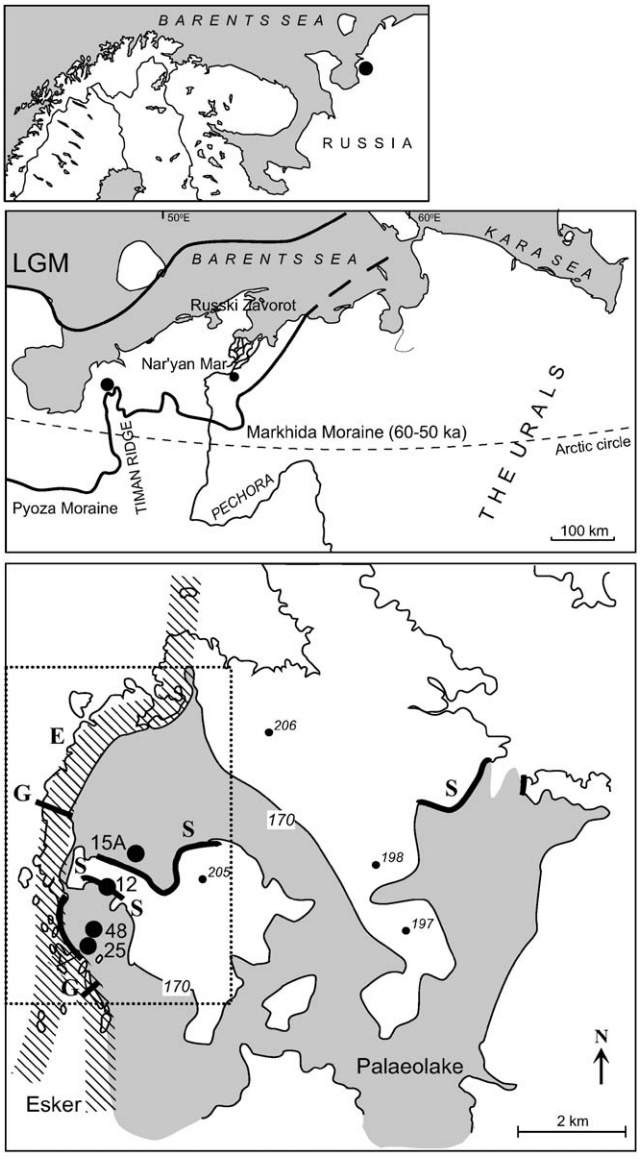


Fig. 1. Maps of different scales showing the study area, coring sites, and names mentioned in the text. The study area and coring sites are shown with large dots. The southern limits of the Barents–Kara Ice Sheet at 60–50 ka and the LGM are indicated (Svendsen et al., 1999, Svendsen et al., submitted). The local map shows the highest level (170 m a.s.l.) of the lateglacial palaeolake (shaded), which is reconstructed by mapped shorelines and stratigraphic observations. In the local map, the stippled outline of Fig. 2 includes the coring sites, the esker (E), the recognised shorelines (S, in bold lines), and two erosional gaps (G) through the esker.

2.2. Sample sites

All the investigated sites are within the margins of Lake Timan. Bolvan I is a round, flat bog of about 1 km^2 in a depression (160 m a.s.l.) delimited by bedrock and glacial deposits. The catchment drains southwards. Coring sites 25 and 48, ca 150 m apart, are located on the *Sphagnum* bogs close to a local pond.

Close to the northern rim of Bolvan I, a distinct shoreline is incised into the silty soil (170 m a.s.l.). Just above and perpendicular to the shoreline, an erosional exposure was cleared (locality 12, Fig. 1).

About 2 km north of Bolvan I, at the head of an erosional ravine, the peat profile of a present *Sphagnum* bog underlain by silt and clay, was exposed at ca 168 m a.s.l. (locality 15A, Figs. 1–3). The studied sequence is located in a small depression on a low esker ridge. Its catchment drains northwards.

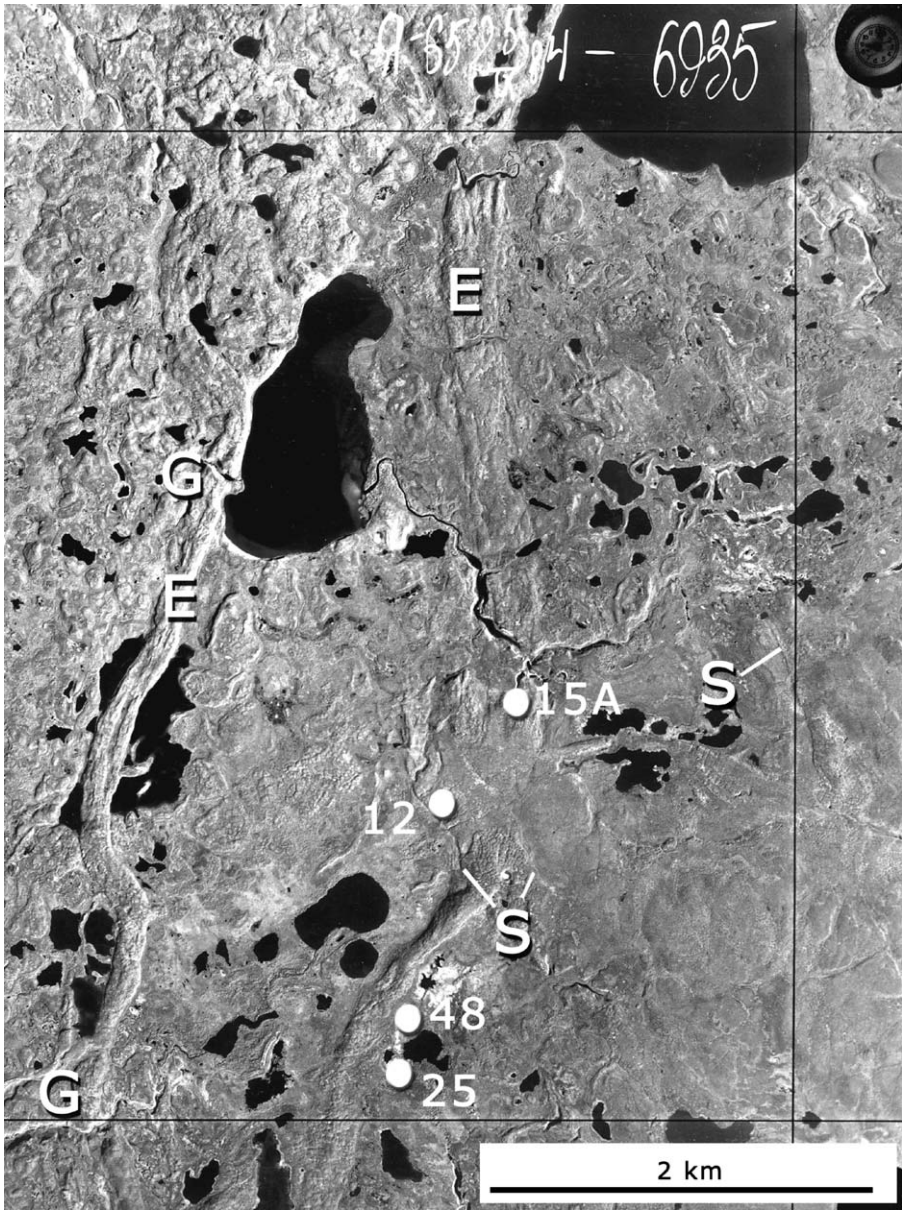


Fig. 2. Aerial photo of the studied area showing the coring sites (12, 15A, 25, 48), the eskers (E), the shorelines (S), and the erosional gaps (G) through the esker that dammed Lake Timan. Notice the hummocky landscape to the west of the damming esker ridge.

2.3. Climate and vegetation

The mean January and July temperatures in the study area are ca −15°C and 9–10°C, respectively (Barents Euro-Arctic Region Databank). At the Barents Sea coast, ca 30 km north of the study area, annual precipitation is 400–450 mm with a peak in August–October (NOAA NCDC GCPS monthly station).

The study area is situated in the Malozemelskaya Tundra within the low Arctic zone. On well-drained elevations and slopes, dwarf-shrub heaths (with e.g. *Betula nana*, *Empetrum*) and herb-rich grasslands dominate. Exposed ridges are lichen-dominated. Snow beds with e.g. *Salix herbacea* are frequent. Willow scrub and tall-herb vegetation are found in protected depressions. *Juniperus communis* is restricted to south-facing and protected slopes.

Wetlands are ombrotrophic *Sphagnum* bogs or fens dominated by *Carex aquatilis* or *Eriophorum russeolum*. A few palsas and turf-tussock formation show frost influence. The area is located within the zone of discontinuous permafrost (Brown et al., 1997).

About 3 km south of Bolvan I, vegetation of *Betula pubescens* reaches its northern limit as table-birch scrubland (sensu Oksanen et al., 1995) on south-facing slopes. According to Kremenetski et al. (1998) and MacDonald et al. (2000a), *Picea* forms the regional treeline in this part of Russia, but *Picea* was not observed here by us.



Fig. 3. The cleared section at site 15A showing the lateglacial lacustrine sequence capped by the Holocene peat. The spade is approximately 1.2 m long. The close up shows from below and upwards: the lateglacial clay, the thin and compressed terrestrial peat of early Holocene age, the olive green gyttja of the shortlasting pond phase, and the stratified peat from the birch-forest phase.

3. Material and methods

3.1. Field work

At Bolvan I, the basin stratigraphy is represented in a transect based on 33 coring sites (Fig. 11) using a 54 mm Russian corer. Sites 25 (Late Weichselian) and 48 (Holocene) were cored for pollen analysis using a 110 and 54 mm Russian corer from the bog surface. The exposed sections at locality 12 and 15A were cleaned, described (Table 1), and sampled for pollen analysis (2–10 cm intervals) and dating.

3.2. Laboratory and analytical work

Pollen samples (1 cm^3) had *Lycopodium* tablets added for estimates of concentration and influx (Stockmarr, 1971) and treated with HF and acetolysed according to Fægri and Iversen (1989). Percentage loss-on-ignition (LOI) or total-organic-carbon (TOC) were estimated.

Pollen identifications were based on Fægri and Iversen (1989), Moore et al. (1991), and Punt et al. (1976–1995), in combination with a reference collection of modern material. Phase contrast/oil immersion objectives ($63\times/1.4, 100\times/1.3$) and $10\times$ oculars were

Table 1
Lithostratigraphical descriptions of the sequences 12, 15A, 25, and 48

Depth (cm)	Material	Colour	Comments
Site 25			
252–299	Fine detritus gyttja (FDG)	Greyish brown	With rootlets, *Equisetum* roots. Lighter and silty in lower part
299–302	Peat	Blackish brown	With rootlets and macro-remains
302–306	Sandy/silty gyttja	Yellow brown	
306–308	Peat	Blackish brown	With twigs and other macro-remains
308–325	Silty gyttja	Brownish grey	With macro-remains and *Equisetum* roots
325–352	Sandy silt	Blueish grey	With low organic content
352–382	Silty clay	Brownish grey	With low organic content
382–528	Compact silt	Blueish grey	With low organic content
Site 48			
0–60	Wet *Sphagnum* peat	Yellowish brown	With roots. Unconsolidated and not sampled
60–150	Fibrous peat	Brown	With *Sphagnum* and roots
150–158	Moss layer	Dark brown	Entirely of *Paludella squarrosa*
158–195	Coarse detritus gyttja (CDG)	Dark brown	With macro remains
195–310	FDG	Brown	Partly grainy and cracked/fissured structure. Macro remains including tree-birch fruits at 305 cm.
310–386	FDG	Brown	With lighter parts
386–387	Silt	Grey	
387–405	FDG	Brown	Lighter in the upper part. Macro-remains
405–410	Peat	Blackish brown	With twigs and other macro-remains
410–414	Sandy peat	Blackish brown	With macro-remains
414–424	Sandy silt	Brownish yellow	With 2–20 mm stones
Site 15A			
0–90	*Sphagnum* peat	Light brown	
90–135	Peat	Dark brown	
135–195	Peat	Reddish brown	Compact and distinctly stratified
195–206	FDG	Olive green	Compact. Leaves of *Betula pubescens* at 200 cm
206–208	Peat	Blackish brown	With catkins and compressed twigs and roots of tree-birch
208–219	Clay	Brownish grey	Upper part sharply delimited and with roots
219–252	Clay	Blueish grey	
252–272	Clayey silt	Brownish grey	
272–295	Sand	Yellow	With silt laminations. Layer of stone/gravel in the lower part
295–325	Silty sand	Grey	
Site 12			
0–10	Minerogenic soil	Dark brown	From present-day dwarf-shrub heath
10–53	Silt	Brownish grey	
53–70	Clay	Blueish grey	Cracked. Lower part of rust-remains of fully oxidised roots
70–160	Sandy silt	Yellowish grey	With oxidised roots
160–180	Sand	Light grey	Low organic. No roots.

used. To objectively separate *Betula nana* pollen from tree-birch pollen, *Betula* pollen grain diameters (Eneroth, 1951) and diameter/pore-depth ratios (Birks, 1968) were measured at selected levels at loc. 15A. One hundred grains per sample were measured to the nearest ocular half-line (0.8 μm). Mounting medium was glycerol.

In the pollen diagrams, the percentage calculation basis ($\sum P$) comprises the terrestrial pollen taxa, including unidentified pollen but excluding the sedges that show local over-representation. For a taxon X within sedges, aquatic pollen, spores, and secondary microfossils, the calculation basis is $\sum P + X$.

The zonation of the pollen diagrams was based on the computer program ZONE 1.2 (S. Juggins, 1991, unpubl.). The computer programs CANOCO 3.12 (Ter Braak, 1987–1992) and CANODRAW 3.0 (Smilauer, 1992) were used for detecting and graphing the ordinational patterns in the terrestrial vegetation development. Palynological richness was estimated by rarefaction analyses (program RAREPOLL, Birks and Line, 1992).

3.3. Dates

Sixteen AMS dates (usually on terrestrial macrofossils), seven conventional radiometric dates (on bulk sediments/peat), and two TL-dates were obtained (see Table 2 and Fig. 4). Age calibration is according to Stuiver et al. (1998).

Table 2
Dating results

Site	Depth (cm)	Material	Lab. ref.	Age BP		$\delta^{13}C$	Method	Comments
				Uncalibrated	Calibrated			
25	252–260	Macros	Beta-116428	3890±90	4425–4155	−24.7	AMS	From gyttja
	294–299	Gyttja	T-11913A	8265±140	9420–9000	−28.2	Conv.	Hardwater/redeposition
	306–307.5	Macros	TUa-1154	7345±75	8165–8010	−27.4	AMS	From peat
	318–323	Org. silt	Beta-116426	10.440±110	12.475–12.175	−25.1	AMS	Hardwater/redeposition?
	320–325	Org. silt	Beta-116425	10.020±90	11.580–11.080	−25.3	AMS	Hardwater/redeposition?
	365–370	Org. clay	TUa-1155A	11.620±105	13.675–13.425	−25.5	AMS	Hardwater/redeposition?
	420–430	Silt	Beta-116427	13.520±110	16.325–16.025	−21.9	AMS	Hardwater/redeposition?
	430–435	Silt	PEC3	11.280±1000			TL	
	495–504	Silt	TUa-989A	20.100±230	24.080–23.540	−24.5	AMS	Hardwater/redeposition
48	60–65	*Salix* twig	Beta-116429	1670±80	1685–1660/1630–1500	−27.5	AMS	From peat. Redeposited?
	150–155	Moss	Beta-116430	1630±50	1555–1485/1475–1435	−21.1	AMS	*Palludella squarrosa.*
	162–167	Gyttja	T-11910A	3060±85	3370–3135	−26.5	Conv.	Hardwater/redeposition
	198–207	Twigs	Beta-116431	4120±60	4820–4530	−27.4	AMS	Vertical mixing by frost
	207–217	Gyttja	T-11911A	6425±100	7390–7220	−22.2	Conv.	Vertical mixing by frost
	287–297	Gyttja	T-11912A	6645±100	7550–7400	−22.8	Conv.	Vertical mixing by frost
	298–308	Macros	Beta-116432	3720±40	4140–3965	−27.4	AMS	Vertical mixing by frost?
	365–370	Gyttja	T-11914A	8180±90	9250–8990	−27.2	Conv.	Hardwater/redeposition
	405–410	Peat	T-11915A	7350±60	8160–8025	−29.2	Conv.	
15A	94.5–95.5	Macros	Beta-116433	4790±60	5600–5465	−24.8	AMS	From peat
	144.5–145.5	Macros	Beta-116434	7250±70	8100–7940	−24.2	AMS	From stratified peat
	149.5–150.5	Macros	Beta-116435	7680±70	8460–8375	−23.5	AMS	From stratified peat
	189.5–190.5	Macros	Beta-116436	8270±80	9380–9040	−26.4	AMS	From stratified peat
	204–205	Gyttja	T-11916A	10.400±100	12.425–12.125	−33.2	Conv.	Hardwater/redeposition
	206	*Betula* twig	Beta-88789	8820±60	9900–9830/9760–9660	−28.6	AMS	From peat
12	53–58	Clay/silt	PEC2	10.220±1040			TL	Shore-line dating

4. Results

4.1. Litho- and chronostratigraphy (Tables 1 and 2)

4.1.1. Bolvan I (160 m a.s.l.)

The lowermost sediments consist of horizontally bedded sand and gravel. Just above this, there is grayish silt/clay, up to 2.3 m thick. This silt/clay is almost sterile, except for the uppermost 20–30 cm showing visible plant remains and increased LOI. Three AMS bulk dates from the silt/clay layer of site 25 show ages of ca 24, 16 and 13.5 cal. ka BP. Hardwater (cf. Olsson, 1979) and/or redeposition (Sutherland, 1980) may have caused too old ages. However, the date of 13.5 cal. ka BP from the upper, slightly more organic level is consistent with its Late Weichselian interstadial (Allerød) pollen-assemblage. Above this, two AMS bulk dates of silt gyttja yielded the ages of 12.3 and 11.3 cal. ka BP. The youngest accords with the pollen stratigraphy showing the onset of the Holocene.

The upper boundary of the silt gyttja is defined by a distinct sand lamina. At most coring sites, it is draped by a 1–2 cm thin peat bed with frequent plant macrofossils, including mosses, compressed twigs, etc. This peat horizon represents a terrestrial surface, and is dated by two AMS dates to 8.1 cal. ka BP.

Above this peat, there is 2–3 m of silty gyttja. The lower part is light-brown fine-detrital gyttja grading upwards into a darker coarse-detrital gyttja. Dates in the range 9.1–3.2 cal. ka BP (Table 2) show that conventionally dated bulk sediments are up to 2.5–3.5 cal. ka older than AMS dated terrestrial macrofossils from about the same level (Fig. 4). We believe that hardwater (Donner et al., 1971, see presence of calciphilous aquatics) and/or redeposition (Björck et al., 1998) have affected the gyttja dates.

At several coring sites, vertical fissures or cracks appeared in the fine-detrital gyttja. At site 48, similarly dated samples (AMS versus conventional dates) gave similar results within the fissured part (depth 195–310 cm, see Table 2). As also indicated by the uniform pollen stratigraphy (paz 48-3), this probably reflects vertical mixing by frost (Paus, 2000), either by downward penetration of frost (Funder and Abrahamsen, 1988) and/or by redeposition from melting bottom ice floating to the surface and carrying frozen layers of sediments torn from the bottom (Nichols, 1967).

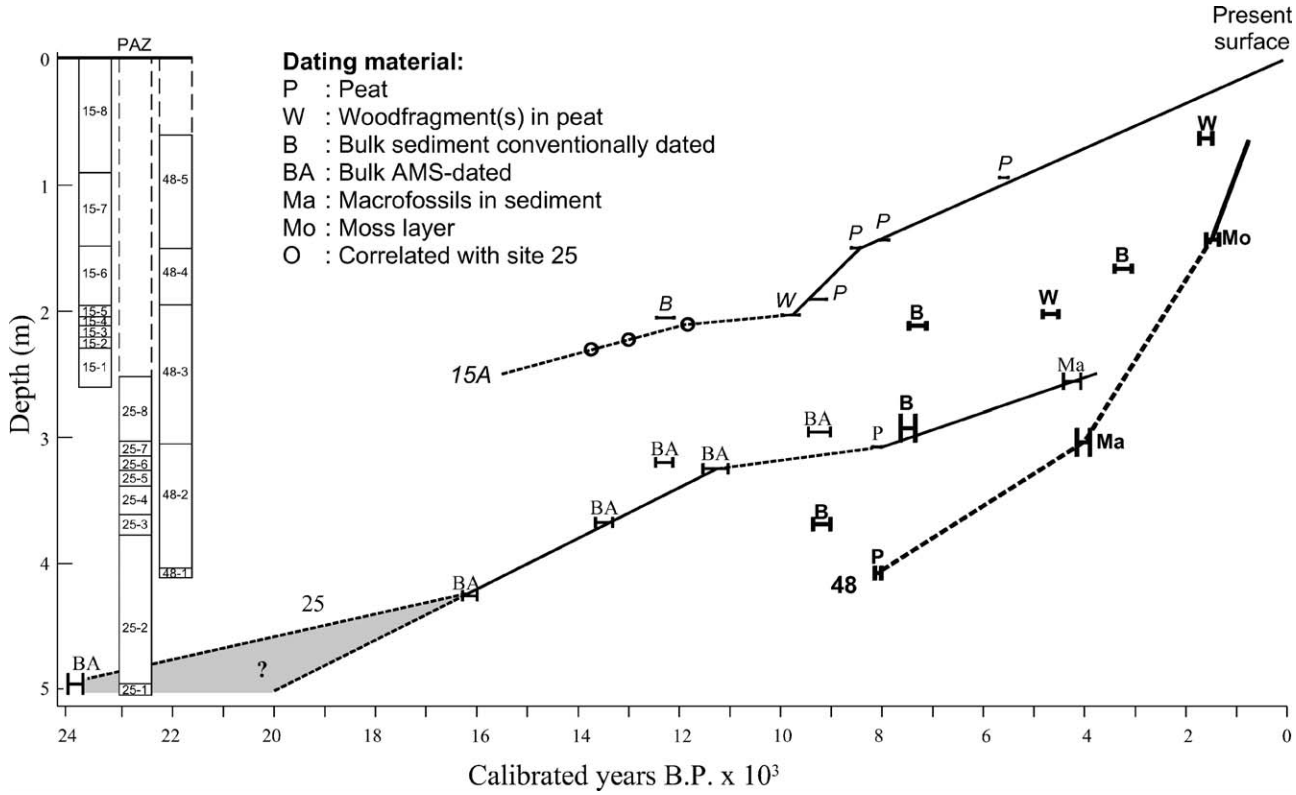


Fig. 4. Dates versus sample depths for sites 15A, 25 (in italics), and 48 (in bold). For each dating sample, the horizontal line shows the date ± one standard error; the vertical lines show sample thickness. Sediment accumulation rates are shown. Stippled lines and shading indicate uncertain rates. At sites 15A and 25, lower rates around 10–12 ka BP indicates hiati/reduced sedimentation during the isolation from Lake Timan.

4.1.2. *Locality 12 (170 m a.s.l.)*

Lowermost is light-grey sand, interpreted as a glaciofluvial deposit related to the adjacent esker system (Figs. 1 and 2). The sand shows a contorted and vague bedding probably caused by cryoturbation. Above follows a 0.5–1.0 m thick unit of sub-horizontally bedded silty sand. It contains frequent, nearly vertical rust-stained structures with a roundish cross-section. They are interpreted as root casts. The sediments contain polished gravel particles of which many were identified as ventifacts. Probably this unit represent a terrestrial soil covered by vegetation. Above, a well-defined, 50–90 cm thick unit of silt/clay, occurs. Its base contains numerous roundish root casts that seems to be water rolled and reworked from the underlying unit. Frequent algae and aquatic pollen throughout indicate that the silt/clay layer is a lacustrine deposit. We assume it reflects a rising Lake Timan that flooded a previous land-surface. Its pollen composition indicates accumulation at the close of the Late Weichselian. A TL date from the middle part of the lacustrine mud yielded the age of $10,220 \pm 1040$ (Table 2).

4.1.3. *Locality 15A (*ca *168 m a.s.l.)*

The base is glaciofluvial sand and gravel, which is part of a broad esker ridge (Fig. 2). The following 2 m sequence of alternating sand and silt layers is capped by a well-defined 0.4 m thick layer of clay. As for locality 12 with similar stratigraphy, we assume that the sediments accumulated at the floor of Lake Timan. Possibly, the upper clay reflects a larger water depth than the sand and silt below. The upper boundary of the clay is sharp and covered by a thin (1 cm) layer of terrestrial peat followed by 10 cm of a dark, olive green gyttja. Above the gyttja, there is a 1.7 m thick sequence of terrestrial stratified peat.

The minerogenic sediments lack any dates. A pre-Holocene age is indicated by pollen-stratigraphical similarities with the dated core 25. Twigs of *Betula pubescens* from the overlying terrestrial peat was AMS dated to 9.8 cal. ka BP. Four levels of the stratified peat above show AMS dates in the range of 9.3–5.5 cal. ka BP.

4.2. *Betula pollen statistics*

The diameter (D) and pore-depth (P) of *Betula* pollen grains were measured from selected levels at site 15A (Fig. 5). The steady diameter increase in paz 15-4 to 15-6 suggest that the pollen size is influenced by depositional processes (Paus, 2000). For this reason, size-independent D/P ratios (Birks, 1968) and curve shapes (Usinger, 1978; Andersen, 1980) are preferred to actual sizes in our interpretation of the *Betula* pollen statistics.

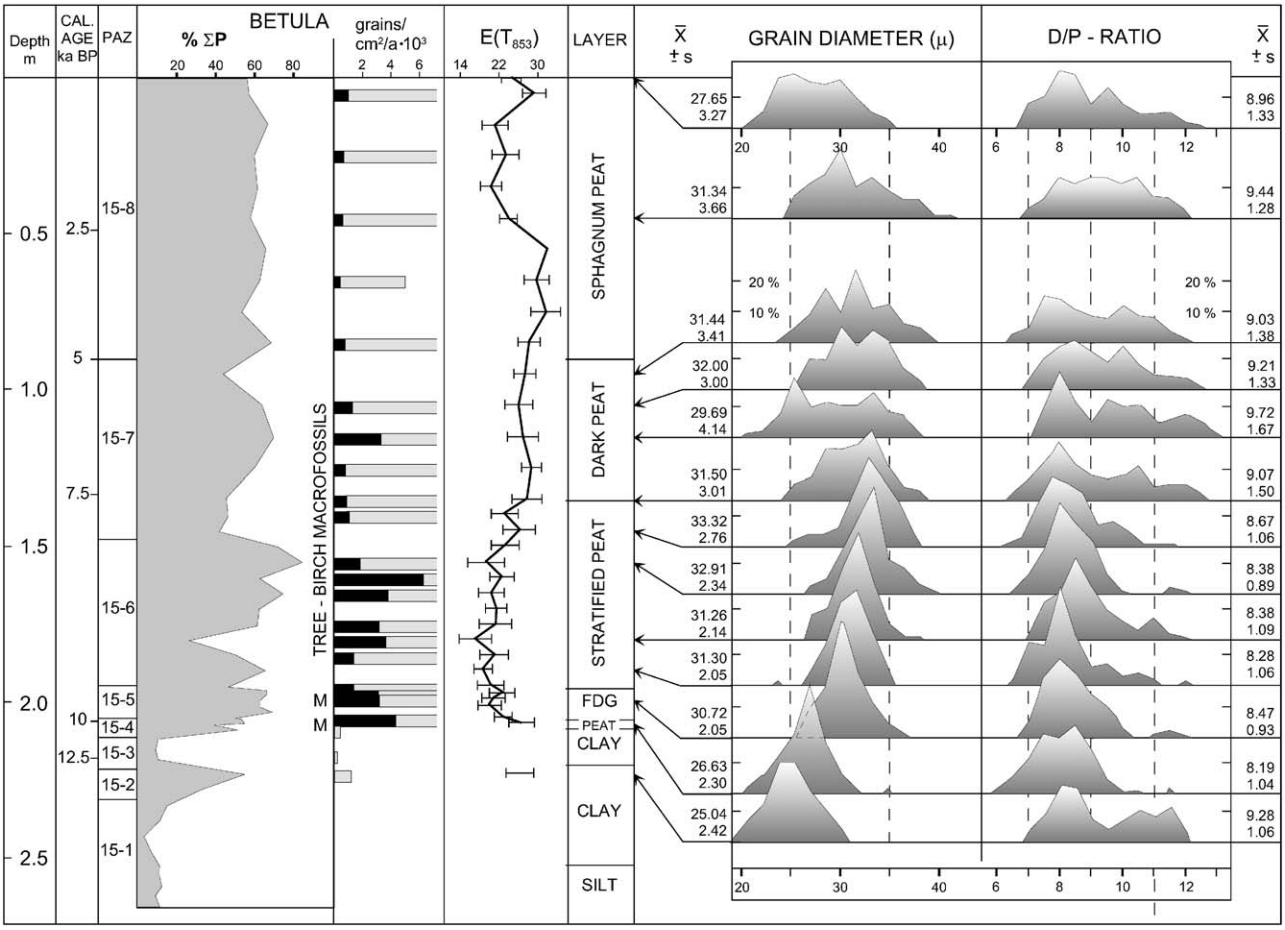


Fig. 5. Results of the *Betula* analysis at site 15A. *Betula* influx (grains cm^{-2} yr^{-1}) and palynological richness estimates ($E(T_{853})$) are also shown. The shaded influx histograms show 10 × exaggeration of the scale. The bars of the richness plots represent the 95% confidence intervals. M denotes finds of tree-birch macrofossils.

In paz 15-4 to 15-6, the *Betula* pollen statistics show unimodal diameter patterns and uniform D/P ratio curves with peaks around 8–8.5. Together with macrofossil finds in paz 15-4 and 15-5 (Table 1, Fig. 5), this indicates the dominance of *Betula pubescens* (cf. D/P ratios of modern *Betula* species; Birks, 1968; van Leeuwaarden, 1982). In paz 15-2, 15-7, and 15-8 and including the surface sample with local *Betula nana*, the curves tend towards bimodal patterns, and the average of the D/P ratios increase, showing simultaneous and distinct representation of both *Betula nana* and tree-birch pollen. The D/P ratios suggest that *Betula nana* pollen constitutes about 1/3 to 1/2 of total *Betula* in these paz.

4.3. Numerical analysis (PCA)

Except for square-root-transformation and down-weighting of rare taxa, default settings in CANOCO were followed. DCA ordination showed the length of the first axis to be 1.865 standard deviation units, indicating linear response curves (Jongman et al., 1987). Hence, PCA was chosen as ordination technique (Fig. 6). Here, pioneer taxa (e.g. *Artemisia*) are distributed to the right. In the upper left of the ordination, tall-herbs (e.g. *Filipendula*), ferns and deciduous trees (e.g. *Populus*), reflecting denser vegetation on fertile humus soils, are concentrated. In the lower left, dwarf-shrubs and other present-day tundra taxa, are found. Here, also conifers and broad-leaved trees appearing as long-distance pollen in modern spectra, are located.

In the ordination of samples, the pollen diagrams (Figs. 8–10) show identical pathways through the ordination space (Fig. 6). The Late Weichselian correlates with the pioneer, mineral-soil taxa on the right. The early Holocene shows affinity to the fertile-soil taxa in the upper left, whereas late Holocene samples relate to the dwarf-shrubs and long-distance taxa in the lower left.

4.4. Palynological richness estimates

The palynological richness is a proxy for the total floristic richness within the pollen source area and

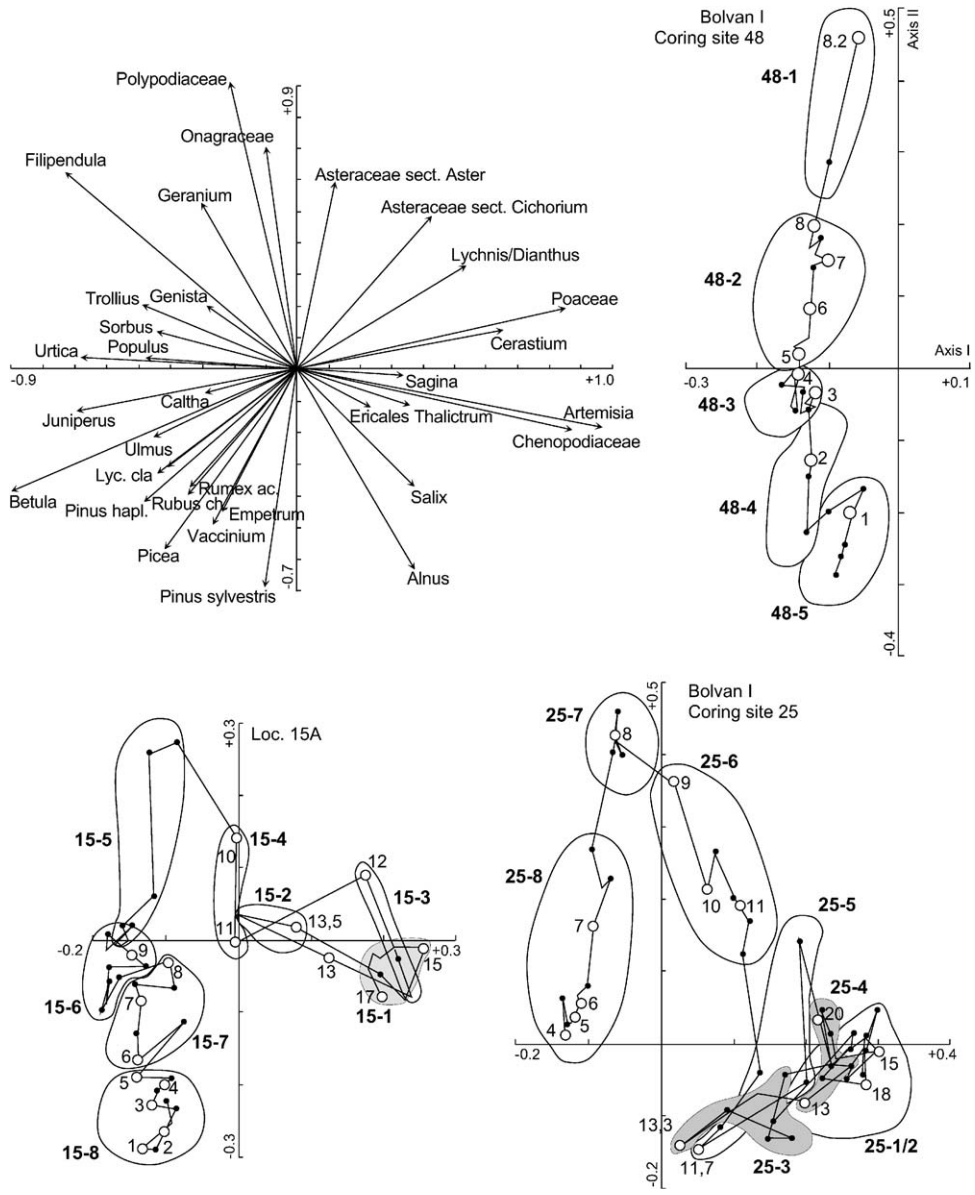


Fig. 6. PCA ordination of pollen types and spectra of the total data set (sites 15A, 25, and 48). Eigenvalues of the first four axes are 0.461, 0.198, 0.072, and 0.054, respectively. The first two axes capture 65.9% of the total data-set variance. Pollen assemblage zones are circled. Small numbers show interpolated ages in cal. ka B.P.

includes the richness of component vegetation types and the mosaic structure within the pollen catchment (Birks and Line, 1992; Odgaard, 1999). Intermediate levels of disturbance maximise richness by preventing both dominance and extinction of species (Grime, 1973).

As the local terrestrial vegetation development is the focus of this study, aquatics, reworked pollen and long-distance dispersed pollen were excluded from the rarefaction analyses (Birks and Line, 1992). The often dominating representation ($2–4 \times \sum P$) of Cyperaceae, *Lycopodium annotinum*, and Polypodiaceae most probably reflect local contamination, so they were excluded from the data set prior to the analyses.

Two series of estimates, $E(T_{404})$ and $E(T_{165})$, were carried out (Fig. 7). $E(T_{404})$, with $\sum P = 404$ as the statistical basis, compares the pollen-rich Holocene samples of the three sites, whereas $E(T_{165})$ compares the Late Weichselian and early Holocene samples of sites 15A and 25 with lower $\sum P$. Due to little pollen and distinctly higher proportions of reworked microfossils, paz 25-1 is not included in the analyses. In the discussion of deforestation, $E(T_{853})$, a more reliable measure of richness than $E(T_{404})$, was estimated at site 15A (Fig. 5).

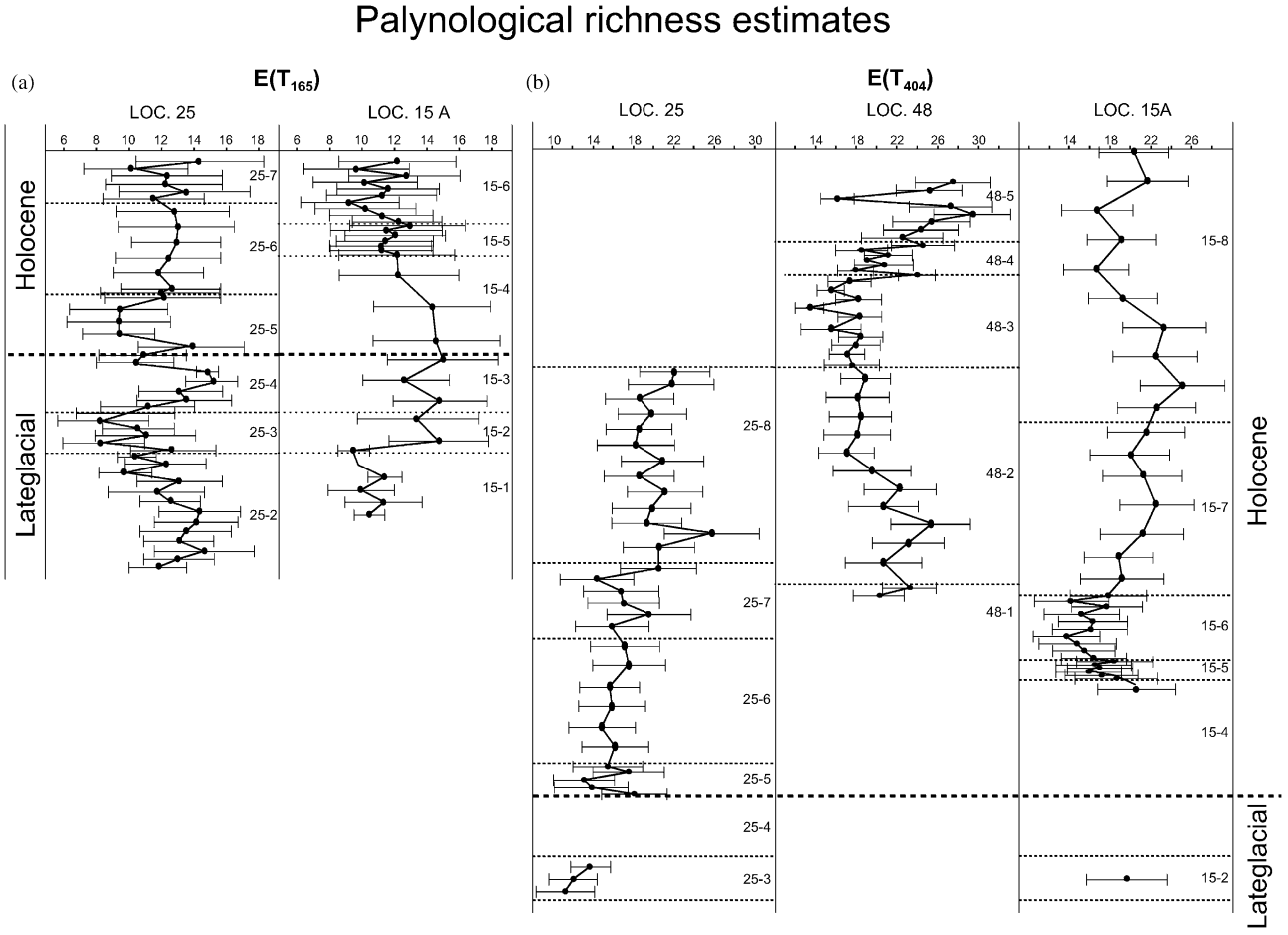


Fig. 7. Palynological richness estimates ($E(T)$) with 95% confidence intervals: (a) $E(T_{165})$ for the Lateglacial/early Holocene; (b) $E(T_{404})$ for the Holocene. The chronological correlated pollen assemblage zones are inserted.

5. Discussion

5.1. Lake history and melting of dead ice (Figs. 1, 2, 11)

The last active ice sheet that covered this region, probably disintegrated some 60–50,000 years ago (Astakhov et al., 1999; Mangerud et al., 1999, 2001). However, the ^{14}C-dates from Bolvan I (core 25) indicate that lacustrine silt/clay started to accumulate on the lake floor as late as 20–15,000 years ago. Our explanation why this lake seems to have formed much later than the regional deglaciation is that large pieces of stagnant glacier ice survived throughout the Middle Weichselian and thereby prohibited any lake formation. In line with this, Astakhov et al. (1999) have shown that buried ice has survived for more than 60,000 years in NE Pechora lowland. As no lacustrine deposits older than 20–15,000 years have been found within the study area, the most intensive melting event probably occurred after the LGM.

We assume that as soon as Lake Timan filled up the entire basin, the out-flow river(s) started to erode the spillways by downcutting through the damming eskers (Figs. 1, 2, 11), causing a lake-level drop. At site 15A, the accumulation of lacustrine clay ceased soon after the transition to Holocene suggesting that the lake became smaller. The basal peat layer above shows that the lake level dropped below 168 m a.s.l. not later than ca 9.8 cal. ka BP. A similar rapid lake-level drop at Bolvan I (160 m a.s.l.) is shown by a pronounced increase of organic content indicating that a shallow local lake developed in the early Holocene. Thereafter, the lake floor of Bolvan I was covered by a thin terrestrial peat at ca 8.1 cal. ka BP.

Gyttja deposits above these peat horizons at both sites show the formation of younger local lakes (Fig. 11). At site 15A, the lake stage was short-lasting (9.8–9.4 cal. ka BP), whereas lakes at Bolvan I have existed since ca 8.1 cal. ka BP up to present. These lakes could have a climatic origin. However, we find it more likely that these ponds formed when the ground subsided due to melting of buried glacier ice that survived for several thousand years underneath the floor of Lake Timan (Fig. 11). At site 15A, this is

indicated by the occurrence of faults and deformation structures within the underlying strata interpreted to show post-depositional sagging.

5.2. The pollen assemblage zones (paz) and local vegetation

5.2.1. Bolvan I, core 25 (Figs. 6–8)

5.2.1.1. Local paz 25-1: Artemisia–Poaceae–Ericales and local paz 25-2: Artemisia–Poaceae–Cyperaceae (before Late Weichselian interstadial). Total pollen influx below 200 grains cm^{-2} a^{-1} compares to modern mid-arctic tundra (Ritchie and Lichti-Federovich, 1967; Fredskild, 1973). A local discontinuous pioneer vegetation on unstable mineral-soils involved wind-blown ridges (cf. *Papaver*, *Achillea*-type) and snow-beds (cf. *Salix*, *Saxifraga*). Whether the wind-pollinated *Artemisia* and Chenopodiaceae reflect local steppe or more regional conditions, is unclear. At the paz 25-1/2 transition, decreasing reworked pollen indicate stabilising soils, and the Cyperaceae increase suggests moister soils and/or improved conditions for the aquatics by warming and/or rising lake-level.

5.2.1.2. Local paz 25-3: Betula–Artemisia (Late Weichselian interstadial). Vegetation closure is indicated by: (1) increased total pollen influx (250–1100 grains cm^{-2} a^{-1}), similar to modern low-arctic pollen rain (Ritchie and Lichti-Federovich, 1967) and slightly lower than from the Fennoscandian low-alpine zone (Hicks, 1994; Alm, 1996), (2) an ordination close to humus soil vegetation (Fig. 6), and (3) decreasing palynological richness (Fig. 7), lower than in the Lateglacial of SW Norway (Paus, 1992) and in the early Holocene of northern Fennoscandia (Seppä, 1998). Paz 25-3 is interpreted to reflect ameliorating conditions passing the level of intermediate disturbance (Grime, 1973) towards increased competition (cf. *Betula* dominance). *Betula* D/P ratio (Fig. 5) in paz 15-2, which correlates to paz 25-3, indicates the development of a dwarf-birch tundra.

5.2.1.3. Local paz 25-4: Artemisia–Poaceae (Younger Dryas). Revertance to pre-interstadial conditions is shown by total pollen influx, reworked microfossils, palynological richness (Fig. 7), and the ordination of pollen assemblages (Fig. 6).

5.2.1.4. Local paz 25-5: Betula–Salix–Artemisia (Younger Dryas/Holocene transition). Vegetation closure at the onset of the Holocene are shown by increasing *Betula* and total pollen influx and decreasing palynological richness. The pollen assemblage indicates developing willow scrub with sparse tall-herbs (e.g. *Filipendula*) and possibly tree-birches (*Betula* influx 350 grains cm^{-2} a^{-1}), at least regionally.

5.2.1.5. Local paz 25-6: Poaceae–Filipendula–Onagraceae, ca *11.3–9.0 cal. ka BP.* Rises in grasses, ferns, tall-herbs, and palynological richness reflect more open conditions, but without the mineral-soil pioneers (e.g. *Artemisia*). As Lake Timan dried out (cf. decreasing algae), a moist, early successional stage appears on the newly exposed basin bottom. This seems to suppress the relative values of the regional pollen rain of e.g. birch and willow.

5.2.1.6. Local paz 25-7: Betula–Filipendula–Polypodiaceae, ca *9.0–7.6 cal. ka BP.* The peat layer reflects the next and drier successional stage on the former bottom of Lake Timan. The local establishment of birch forests (*Betula* influx 1000–3000 grains cm^{-2} a^{-1}) included *Populus*, *Sorbus*, tall-herbs and ferns.

5.2.1.7. Local paz 25-8: Betula–Juniperus–Picea, ca *7.6–4.0 cal. ka BP.* Detrital gyttja with abundant aquatics shows the development of a local lake. As this caused an increased pollen source area, palynological richness increased (cf. Birks and Line, 1992; Seppä, 1998), long-distance representation (e.g. *Pinus*, *Picea*, *Alnus*) improved, and pollen influx decreased (cf. Pennington, 1973). The *Betula* influx of 7–800 grains cm^{-2} a^{-1} still suggests local birch-trees (Hyvärinen, 1976; Hicks, 1994; Paus, 1995).

5.2.2. Bolvan I, core 48 (Figs. 6, 7, 9)

5.2.2.1. Local paz 48-1: Betula–Filipendula–Cyperaceae, ca *8.2–8.0 cal. ka BP, and local paz 48-2: Betula–Juniperus,* ca *8.0–4.0 cal. ka BP.* These reflect the same tree-birch/tall-herb stage as paz 25-7/25-8, as visualised by the ordination (Fig. 6). Tree-birch fruits are found at the transition to paz 48-3.

5.2.2.2. Local paz 48-3: Betula–Thalictrum, ca *4.0–2.3 cal. ka BP.* This is comprised by the fissured gyttja, vertically mixed by frost. At its base, the AMS date of terrestrial macrofossils represents a maximum age as fossils probably are reworked or moved upwards by frost. The fissured pattern, the uniform pollen content and the maxima of *Thalictrum* and *Persicaria amphibia* indicate that the frost disturbance is mainly restricted to this paz.

5.2.2.3. Local paz 48-4: Betula–Juniperus–Salix, ca *2.3–1.7 cal. ka BP.* Sudden changes in pollen concentrations and the pollen assemblage in a coarser textured gyttja with roots point to reduced frost mixing (cf. Paus, 2000). The higher palynological richness including taxa diagnostic of tundra, such as *Empetrum*, *Ledum*, *Veratrum*, and *Bistorta*-type, reflect a tundra rather similar to the present. Polypodiaceae, not present today, and *Filipendula*, indicative of fertile soils, gradually decrease.

5.2.2.4. Local paz 48-5: Betula–Salix–Sphagnum, ca *1.7–0.6 cal. ka BP*. The transition from gyttja to *Sphagnum* peat shows a more locally influenced pollen/spore deposition, as visualised by the increase of e.g. *Vaccinium*-type and *Melampyrum*. A more open local vegetation is shown by rising palynological richness (Birks and Line, 1992; Seppä, 1998), improved long-distance representation (e.g *Pinus* spp., *Artemisia*), and increased Poaceae values. The paz, closely ordinated with modern surface samples (Paus, 2000), reflects a tundra similar to the present.

5.2.3. Locality 15A (Figs. 5, 6, 7, 10)

5.2.3.1. Local paz 15-1: Artemisia–Poaceae–Pinus (before the Late Weichselian interstadial, correlated with site 25). This shows a pre-interstadial steppe-tundra similar to paz 25-1/2. However, taxa indicating moister soils/snow beds (e.g. *Caltha*-type, *Rumex*, *Salix*) are absent or less frequent, resulting in lower palynological richness (Fig. 7). A more arid and homogenous vegetation than at the protected site 25 seems to have been formed.

5.2.3.2. Local paz 15-2: Betula–Salix–Ericales (Late Weichselian interstadial, correlated with site 25). Vegetation closure is shown by increasing dwarf-shrubs and tall-herbs and decreasing mineral-soil taxa. Estimated total pollen influx is ca 200 grains cm^{-2} a^{-1} comparable to modern mid-/low-arctic values (Ritchie and Lichti-Federovich, 1967; Fredskild, 1973). As Lake Timan was large, these records may be under-estimates compared to the later basin stages (cf. Pennington, 1973). Hence, the *Betula nana* influx of ca 50 grains cm^{-2} a^{-1} (Fig. 5) reflects local dwarf-shrub tundra, whereas the similar tree-birch influx is too low to indicate local occurrence (Paus, 1995; Alm, 1996). The increasing palynological richness (Fig. 7) involves new taxa on moister soils (e.g. *Caltha*-type, *Koenigia*). Probably, climate reached an optimal disturbance level and increased the number of local habitats.

5.2.3.3. Local paz 15-3: Artemisia–Salix–Dryas (Younger Dryas). The ordination suggests a vegetation break-up and recurrence to the pre-interstadial steppe-tundra conditions (Fig. 6). However, both moist-soils (cf. *Salix*, Cyperaceae) and drained-soils (cf. *Astragalus*, *Dryas*) habitats were still locally present and included new colonists, so the palynological richness shows little change. Apparently, the conditions were still at intermediate disturbance level and were, thus, less harsh than in paz 15-1.

5.2.3.4. Local paz 15-4: Betula–Salix–Empetrum, ca *11.7–9.8 cal. ka BP*. The rapid displacement towards humus-soils in the ordination (Fig. 6), increasing pollen influx, and decreasing palynological richness show a vegetation closure caused by the early Holocene warming. Tree-birch macrofossils (Table 1), D/P ratios similar to modern pollen of *Betula pubescens*, and *Betula* influx of ca 4000 cm^{-2} a^{-1} (Fig. 5) show local birch-forests (Hicks, 1994; Alm, 1996).

5.2.3.5. Local paz 15-5: Betula–Juniperus–Filipendula, 9.8–9.4 cal. ka BP. The gyttja reflects a short-lived pond phase with maxima of *Equisetum* and aquatics. Low D/P ratios, high influx estimates, and leaf fragments show local *Betula pubescens* forests. *Populus* and decreases in Poaceae and palynologial richness suggest a further closing of vegetation. Juniper probably replaced the dwarf-shrubs in well-drained, open areas.

5.2.3.6. Local paz 15-6: Betula–Sorbus–Potentilla, 9.4–8.2 cal. ka BP. Local birch-forests (cf. *Betula* influx, D/P ratios) were of a fern-rich tall-herb type. The minima in *Juniperus*, Poaceae, and palynological richness, and the distinct representation of *Populus*, and *Sorbus* suggest developing shade and increased competition within the forests. At the coring site, moist soils and peat with e.g. *Caltha*, and *Sphagnum* developed.

5.2.3.7. Local paz 15-7: Betula–Juniperus–Poaceae, 8.2–5.0 cal. ka BP. At the lower zone boundary, local deforestation is shown by: (1) *Betula* and other deciduous trees decrease, and the light-demanding *Juniperus*, Poaceae, and long-distance representation increase. The following short-lived NAP maximum parallels similar maxima found by Aario (1940) and Simonsen (1980) to reflect tree-line situations. (2) The *Betula* influx falls to about 1000 grains cm^{-2} a^{-1}, of which one third to one half is *B. nana* (Fig. 5). Both the influx and D/P values are similar to the present tundra (Fig. 5). (3) The palynological richness rise (Figs. 5 and 7) indicates more open conditions (Birks and Line, 1992; Odgaard, 1994). Seppä (1998) also found a richness increase during the Holocene tree-line retreat in Fennoscandia. In paz 15-7, present-day tundra taxa (e.g. *Bistorta*-type, *Empetrum*, *Ledum*) arrive and/or increase, whereas *Filipendula* and *Urtica* on fertile soils decrease. All this suggest deteriorating conditions causing local deforestation, leaching of soils, and the development of juniper-scrub, dwarf-shrub heath and herb-rich grasslands as parts of a mosaic vegetation.

5.2.3.8. Local paz 15-8: Betula–Pinus–Sphagnum, ca *5.0 cal. ka BP - present*

Taxa of the present tundra appear (e.g. *Dianthus*, *Polemonium*, *Veratrum*). A vegetation similar to the present develop already at the zone boundary according to spectra closely ordinated with modern surface samples (Paus, 2000). An early maximum in palynological richness could indicate deteriorating conditions that passed the intermediate level of disturbance. A harsher climate could also have reduced the overall local

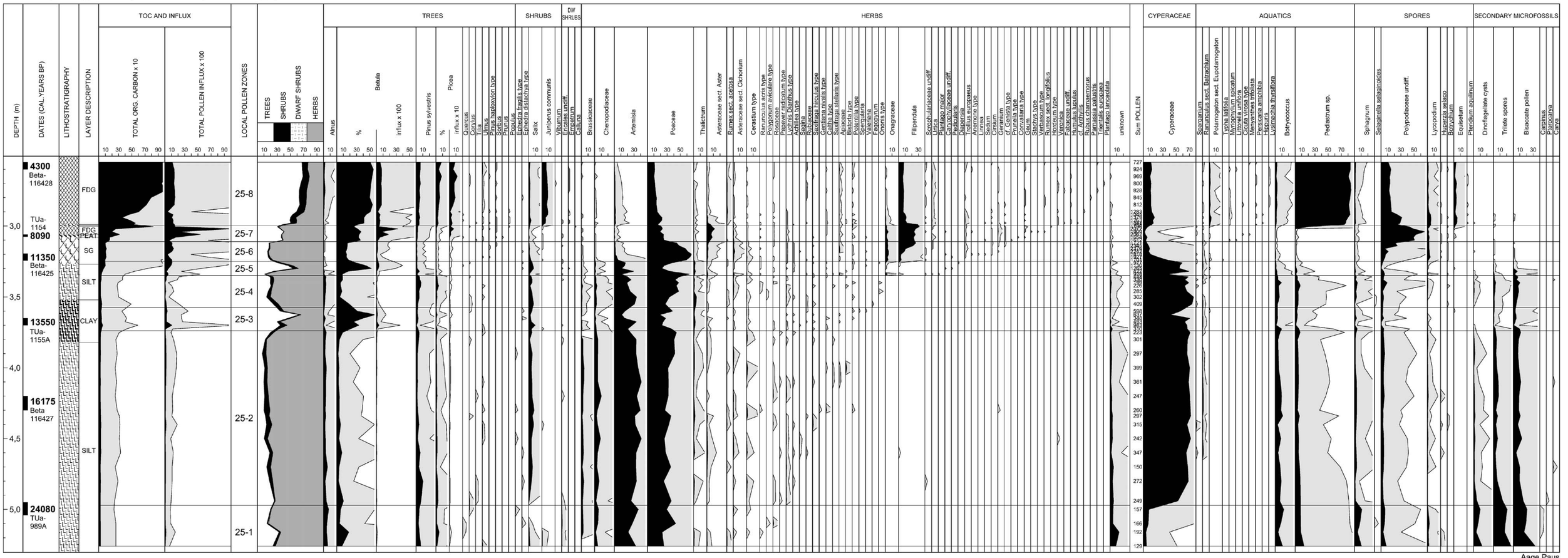


Fig. 8. Pollen percentage diagram of coring site 25 at Bolvan I. Shaded curves are 10 × exaggeration of the scale. Total pollen, *Betula*, and *Picea* influx (grains cm^{-2} yr^{-1}) are also shown.

Bolvan I, coring site 48, 160 m a.s.l., Timan ridge, northern Russia.

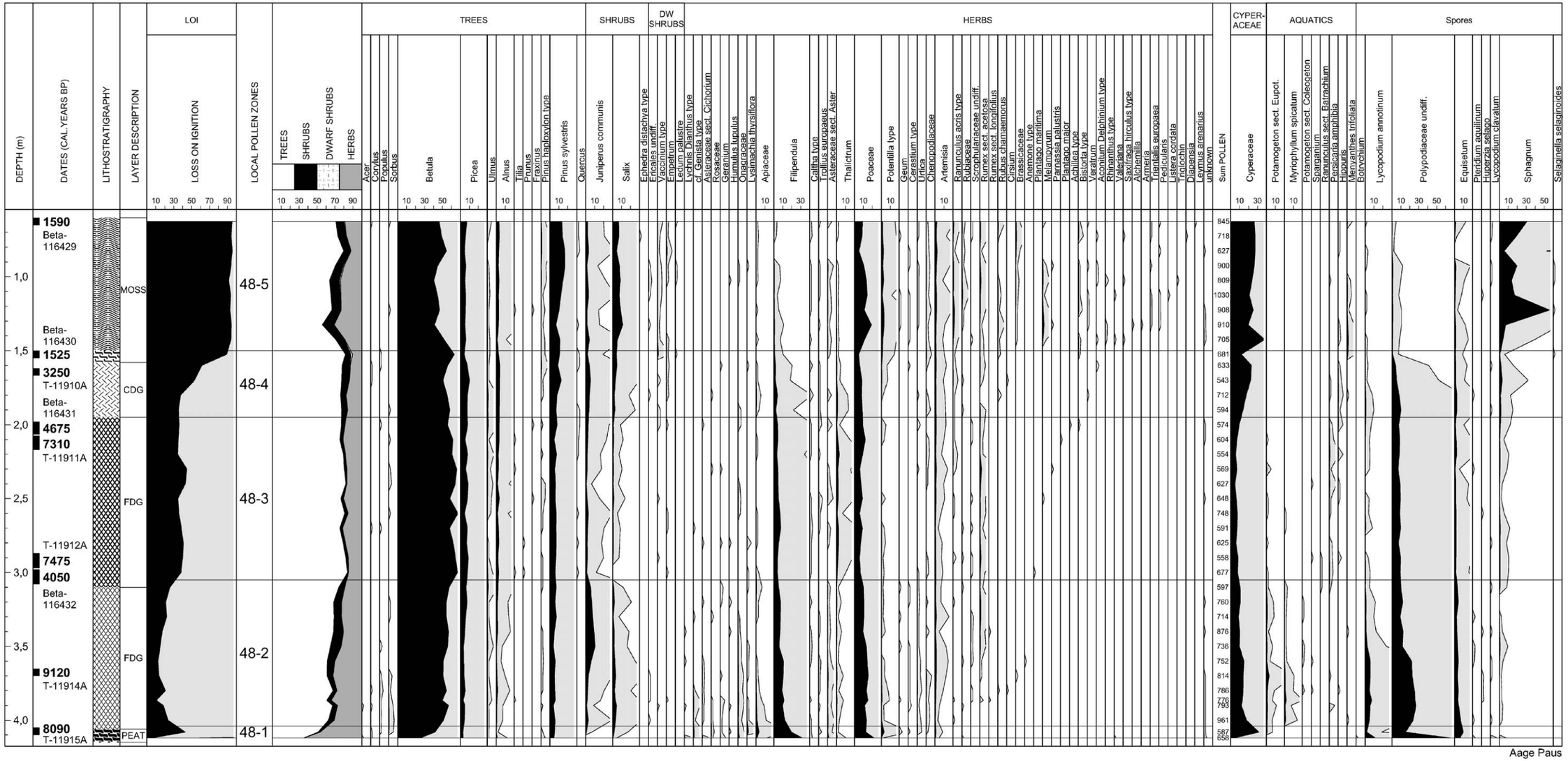


Fig. 9. Pollen percentage diagram of coring site 48 at Bolvan I. Shaded curves are 10 × exaggeration of the scale.

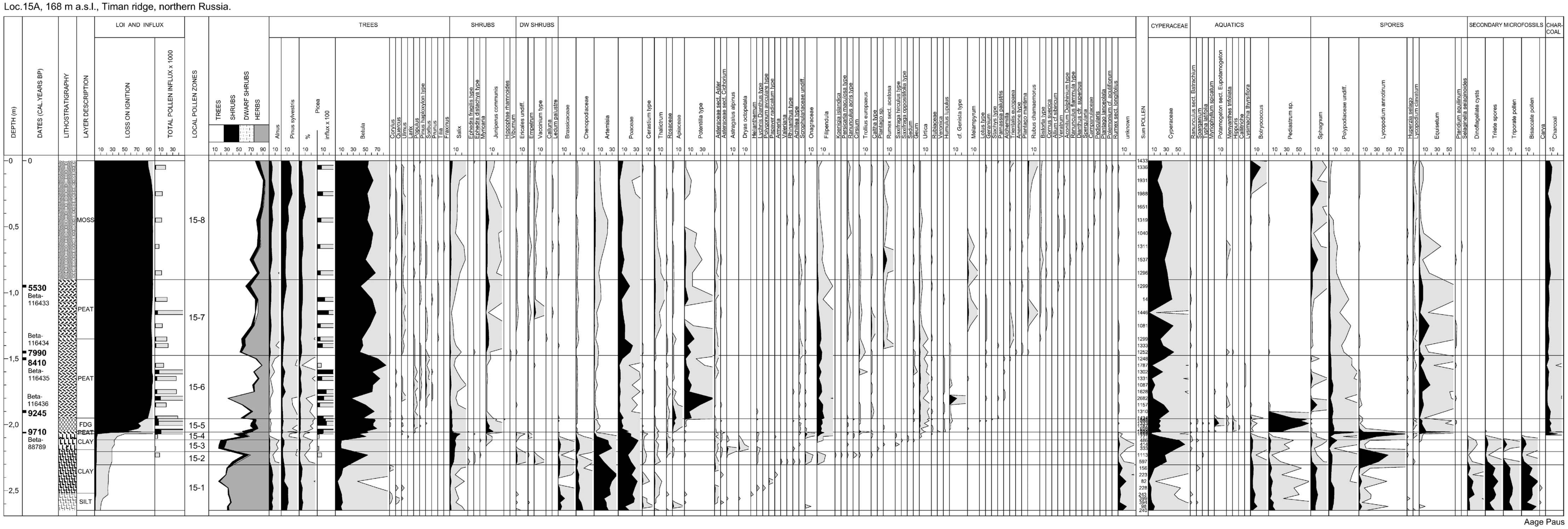


Fig. 10. Pollen percentage diagram of loc.15A. Shaded curves are 10 × exaggeration of The scale. Total pollen and *Betula* influx (grains cm^{-2} yr^{-1}) are also shown.

pollen production and dispersal (cf. Birks and Line, 1992; Moe, 1998). In line with this, long-distance taxa (e.g. *Alnus*, *Artemisia*, *Pinus*) increase, and the present dominant dwarf-shrub heath, except for *Betula nana*, is hardly represented in the surface samples (Fig. 10 and Paus, 2000).

5.3. The regional vegetation and climate history

5.3.1. The Late Weichselian

The pre-interstadial paz 15-1, 25-1 and 25-2 visualise a discontinuous mineral-soil vegetation in a mosaic with e.g. *Rumex*, *Saxifraga*, and *Ranunculus* species on moister soils or in snow beds, and with e.g. *Armeria*, *Dryas*, and *Papaver* on windblown ridges. Mesophytes show distinctly lower representation at the exposed site 15A than at the more sheltered Bolvan I. Together with the well-represented *Artemisia*, Chenopodiaceae and Poaceae, significant similarities with the Late Weichselian steppe/tundra recorded from NW Europe to east of the Urals (e.g. Berglund et al., 1994; Birks et al., 1994; Walker et al., 1994; Hahne and Melles, 1997, 1999; Kondratiene, 1998; Satkūnas and Kondratiene, 1998) appear. Along this periglacial belt, macrofossils show that the wind-pollinated *Artemisia* had some local significance (Webb and Moore, 1982; Kienast et al., 2001).

At Timan, the distinct *Betula* rise, ca 13.8 cal. ka BP, reflects the onset of the interstadial warming. *Betula* pollen statistics and influx estimates (Fig. 5) indicate that this rise reflects local *B. nana* and long-distance tree-birch pollen. Hence, no trees established in the Timan area. This contrasts Khotinsky (1984), Borisova and Zelikson (1995), Zelikson (1997), and Serebryanny et al. (1998), stating that an interstadial forest-tundra established at the Russian Arctic Coast. At Timan, the dominant vegetation type was dwarf-shrub heath with e.g. *B. nana*, Ericales species and *Lycopodium annotinum*. More protected were willow/tall-herb communities (with e.g. *Filipendula*, *Trollius*) and snowbeds (with e.g. *Caltha*-type, *Koenigia*, Onagraceae). Different interstadial patterns of palynological richness changes at sites 15A and 25 (paz 25-3 versus paz 15-2, Fig. 7a) indicate that the sites experienced different levels of disturbance (sensu Grime, 1973). At site 25, reduced richness suggests increased competition, causing a homogeneous dwarf-shrub dominated vegetation. At the exposed site 15A with a northern aspect, however, milder interstadial conditions caused a richness rise by allowing the development of moister habitats locally.

That Lake Timan did not form until the final stage of the Lateglacial, indicate that no major melting event occurred prior to the Late Weichselian interstadial. Hence, this interstadial was probably warmer and more humid than the Middle Weichselian interstadial(s). Inferred from pollen indicators (Table 3), the Lateglacial interstadial warming was only slight with July temperatures similar to present (Fig. 12). In contrast, Velichko (1995), Klimanov (1997), and Kutzbach et al. (1998) infer 4–5°C higher temperatures in the North-Russian interstadial than in other Lateglacial periods. At Timan, a single interstadial tetrad of *Typha latifolia*, indicating a July mean of 13.5°C (Iversen, 1954; Aalbersberg and Litt, 1998), is probably long-dispersed, though rather small amounts of conifer pollen throughout the Lateglacial (Figs. 8 and 10) suggest limited long-distance pollen representation. Probably dominant winds came from glaciated areas in the west and north during summers.

Table 3
Indicator species and their July temperature requirements according to Kolstrup (1979), Paus (1992), and Aalbersberg and Litt (1998)

Typha latifolia	13.5°C
Hippophaë rhamnoides	11.5°C
Betula pubescens	10°C
Myriophyllum spicatum	10°C
Persicaria amphibia	9.5°C
Juniperus communis	8°C
Calluna vulgaris	8°C
Urtica dioica	8°C
Filipendula ulmaria	8°C
Caltha palustris	8°C
Menyanthes trifoliata	8°C
Ranunculus sect. Batrachium	7.5°C
Myriophyllum alterniflorum	7.5°C
Betula nana	7°C
Parnassia palustris	7°C
Selaginella selaginoides	7°C
Trollius europaeus	6.5°C
Bistorta vivipara	5°C

Paz 15-3 and 25-4 reflect the revertance to the mosaic and fragmented pre-interstadial vegetation on unstable mineral soils. We interprete these changes to reflect the Younger Dryas cooling. The Pereslavl' cooling (Khotinsky, 1984) correlated to the Preboreal oscillation (Björck et al., 1997), also shows rises in *Artemisia* and Chenopodiaceae. However, in Russian pollen diagrams recording both periods (Elina et al., 1995; Hahne and Melles, 1997; Khotinsky and Klimanov, 1997; Arslanov et al., 1999), the Younger Dryas pollen assemblage changes are similar to paz 15-3 and 25-4 and distinctly more extensive than for the Pereslavl' event.

5.3.2. The Holocene

Rapid palynological rate of change towards humus-soil vegetation in the ordination (Fig. 6) reflect the onset of the Holocene warming. On the northern part of the Timan Ridge (Fig. 11), birch forests with *Populus*, *Sorbus*, tall-herbs, and ferns developed. Macrofossils at the site 15A show that tree-birch established locally not

later than 9.8 cal. ka BP. In contrast to the Timan records, mixed forests including significant *Larix* and *Picea*, reached the Arctic coast elsewhere (Kremenetski et al., 1998; Kaakinen and Eronen, 2000; MacDonald et al., 2000a). These regional differences is explained by the higher altitude and harsher conditions on the Timan Ridge than in the lowland areas at the same latitude.

In the first half of the Holocene, a July mean of at least 10°C is estimated for the study area (Fig. 12). Long-distance tetrads of *Typha latifolia* (Fig. 12) and birch forests reaching a maximum density in paz 15-6 (Fig. 5), point to a thermal maximum (July) well before 8200 cal. years BP. This accords with studies from present coastal and island areas in Arctic Russia (e.g.

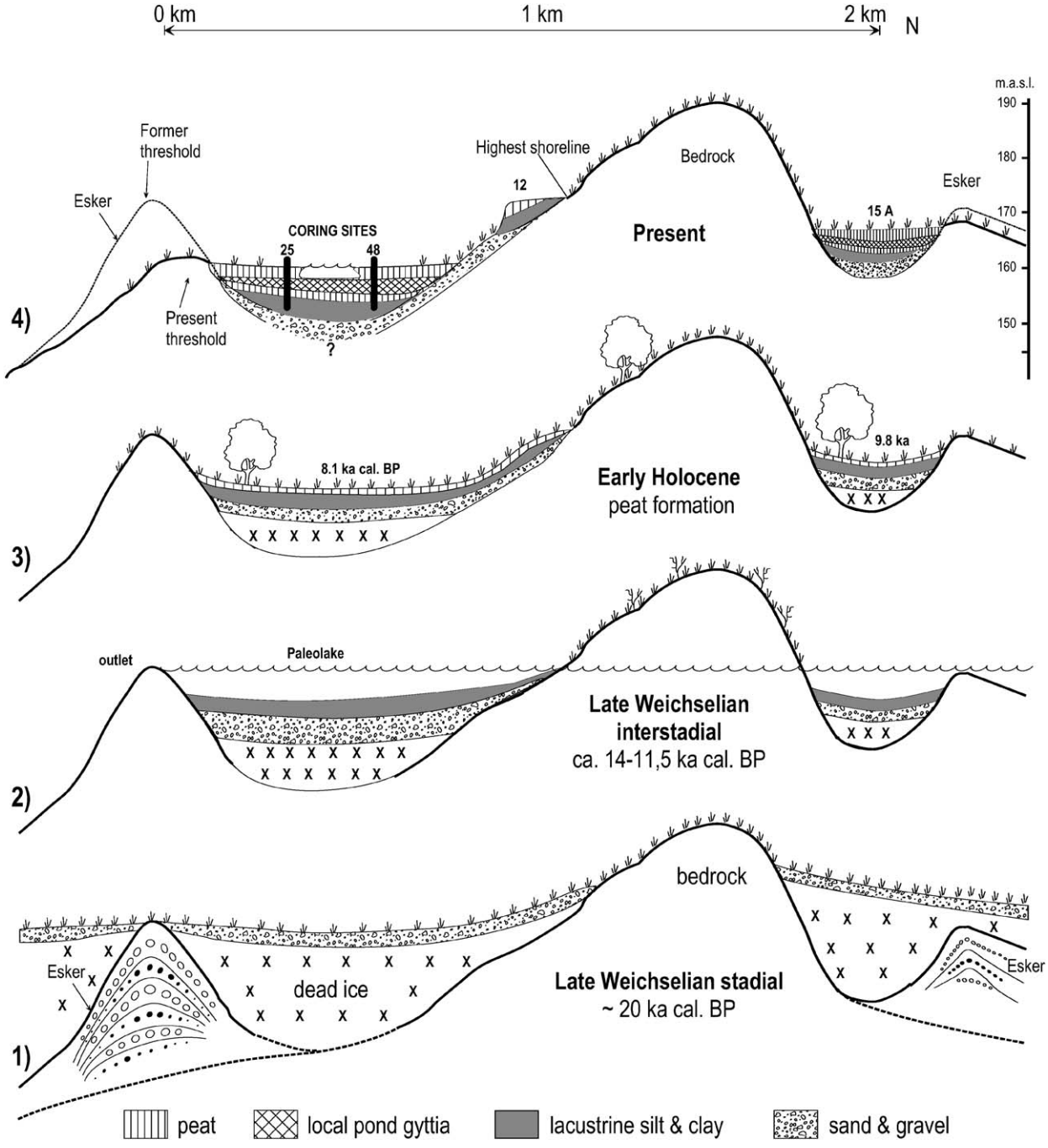


Fig. 11. The interpreted lake development during the lateglacial and the Holocene in the study area of the Timan Ridge. (1) The area was covered by dead ice from the Middle Weichselian deglaciation around 50 ka until the lateglacial warming. (2) A large palaeolake formed during the lateglacial interstadial due to melting of buried glacial ice. (3) A thin terrestrial peat layer formed after the drainage of the palaeolake. (4) The present-day situation with bogs and local ponds. The sampled sites is inserted.

Andreev et al., 1997; Hahne and Melles, 1997, 1999; Serebryanny et al., 1998; MacDonald et al., 2000a). The northernmost finds of tree-birch macrofossils north of the present Russian Arctic treeline (Kremenetski et al., 1998; MacDonald et al., 2000a) also indicate an early Holocene thermal maximum. However, a mid-Holocene maximum is recorded at Russian inland sites (e.g. Elina et al., 1995; Davydova and Servant-Vildary, 1996; Khotinsky and Klimanov, 1997).

At the exposed site 15A, the local deforestation occurs ca 8200 cal. years. Thereafter, this local area remained tree-less throughout the Holocene (Fig. 5). High *Lycopodium* and Polypodiaceae percentages (Figs. 8–10) indicate that these early birch-forests were of an oceanic type (cf. Seppä and Hammarlund, 2000). Furthermore, in the early Holocene, northern Russia experienced wet conditions persisting until at least 7000 ^{14}C years BP (Harrison et al., 1996; Wolfe et al., 2000). Hence, the birch decline at 8200 cal. years (7500 ^{14}C years) BP was probably not caused by increasing aridity (cf. Kullman, 1986; MacDonald, 1993). The initial deforestation is simultaneous with a pronounced cooling (8200-event) recorded in Greenland ice cores (Johnsen et al., 1992) and which seems to have had global impact (Dahl and Nesje, 1996; Alley et al., 1997; Stager and Mayewski, 1997; Haas et al., 1998). This event has been related to changes in the North-Atlantic ocean-atmospheric system (Klitgaard-Kristensen et al., 1998; Dean et al., 2002). As the Russian Arctic are influenced by incursions of North-Atlantic air (Rogers and Moseley-Thompson, 1995; MacDonald et al., 2000b), this cooling could have affected northern European Russia. In contrast to global records, no evidence suggests a climatic warming after the 8200 cooling on the Timan Ridge.

Contrasting the site 15A records, Bolvan I shows a gradual birch-rise in the first half of the Holocene. Then, at the paz 48-3/48-4 transition, the same palynological patterns (Figs. 6 and 7) appear as recorded at the deforestation in the 15A peat. We interpret this zone transition to reflect the regional deforestation, as it is recorded in lake gyttja and by more gradual pollen-assemblage changes than at site 15A. AMS-dated terrestrial macrofossils at the base of paz 48-3 give the maximum date of ca 4000 cal. years BP for initiation of the deforestation. This approaches the dates for treeline retreat elsewhere in northern Eurasia (3–4000 cal. years BP; Kaakinen and Eronen, 2000; MacDonald et al., 2000a). Thus, a time-lag of at least 4000 cal. years is indicated between the local deforestation at locality 15A and the regional deforestation at the more sheltered Bolvan I ca 2 km further south (see Fig. 6). It should be noted that one single specimen of *Betula pubescens* is still surviving on Bolvan I, and that the present northern limit of tree-birch vegetation is situated about 3 km to the south of Bolvan I and

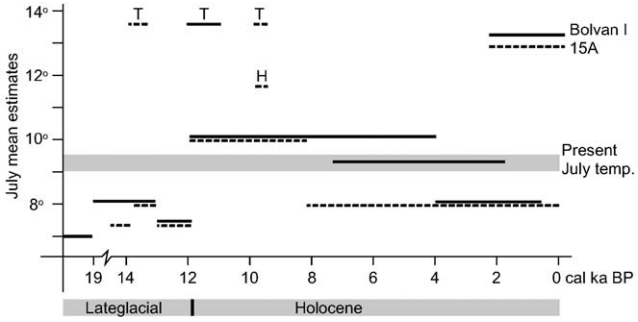


Fig. 12. July temperatures inferred from the indicator species in Table 3. The difference between the estimated and meteorologically measured present-day July means shows that the indicated temperatures are minimum estimates. Temperatures indicated by long-distance pollen grains/tetrads of *Hippophaë* (H) and *Typha latifolia* (T) are added.

restricted to south-facing slopes. This irregular shape of the present tree-line suggests that the former tree-line did not retreat as a southerly moving front. As today, its shape was most likely topographically determined. Exposed sites, such as site 15A, were deforested early, whereas south-facing and protected sites retained tree-birch vegetation much longer. The present *Salix* vegetation may be an analogue to the former tree-birch vegetation. Willow-shrubs are found in depressions and along river courses reaching the Barents Coast, but are absent from higher sites and ridges within the study area 30–40 km further south.

6. Conclusions

1. A ca 20 km^2 large paleolake (Lake Timan) formed on the Timan Ridge during the Late Weichselian as a response to a pronounced climatic warming and increased precipitation. This lake was drained during the early Holocene as the out-flow rivers rapidly eroded the spillways. The present lake basins are kettle holes formed during the Holocene when buried glacier ice melted.
2. The following vegetation development was reconstructed within the study area: (a) a pre-interstadial discontinuous vegetation on unstable mineral-soils with xerophytes and mesophytes in topographically determined mosaics, (b) a Late Weichselian interstadial dwarf-shrub tundra dominated by *Betula nana*, (c) a Younger Dryas mineral-soil vegetation similar to the pre-interstadial, though snow-beds were better represented, (d) early to mid Holocene birch-forests with *Populus*, *Sorbus* and tall-herbs, and (e) a gradual development into the present tundra mosaics of dwarf-shrubs, grasslands, and willow-shrubs with tall-herbs.

3. The Holocene thermal maximum was reached earlier than 8200 cal. yr BP. At this time, the tree-line started to retreat whereas the regional deforestation of the Timan Ridge was completed at least 4000 years later. A gradual climatic cooling after 8200 cal. yr BP is reflected.
4. Local differences in the vegetation history appear between the exposed site 15A, and the sheltered Bolvan I, 2 km further south. In contrast to Bolvan I, site 15A shows: (a) minor representation of mesophytes in the pre-interstadial, (b) a better-developed mosaic vegetation with high palynological richness in the Late Weichselian interstadial, (c) a distinct earlier tree-line retreat in the Holocene.
5. The palynological records from Timan ridge at a high altitude contrast studies from the Russian Arctic lowland by showing: (a) cooler summers and no forests in the Late Weichselian interstadial, (b) scarce or absent *Picea* and *Larix* in the Holocene forests, and (c) an early initiation of the Holocene deforestation.

Acknowledgements

This paper is a contribution from the Russian-Norwegian interdisciplinary project "*Paleo Environment and Climate History Of the Russian Arctic* (*PECHORA*)" financially supported by the Norwegian Research Council. We thank Jan Berge for preparing the pollen samples, Beate Ingvartsen for drawing of the figures, and John Birks for commenting on an earlier manuscript version.

References

Aalbersberg, G., Litt, T., 1998. Multiproxy climate reconstructions for the Eemian and early Weichselian. Journal of Quaternary Science 13, 367–390.

Aario, L., 1940. Waldgrenzen und subrezente Pollenspektern in Petsamo Lappland. Annales Academia Scientarium Fennica A 54.8, 1–120.

Alley, R.B., Mayewski, P.A., Sowers, T., Stuiver, M., Taylor, K.C., Clark, P.U., 1997. Holocene climatic instability: a prominent, widespread event 8200 yr ago. Geology 25, 483–486.

Alm, T., 1996. Pollen influx in traps along a height transect on mount Ädjit, Troms, northern Norway. In: Frenzel, B. (Ed.), Holocene Treeline Oscillations, Dendrochronology and Palaeoclimate, Paläoklimaforschung 20, 157–171.

Andersen, S.T., 1980. Early and Late Weichselian chronology and birch assemblages in Denmark. Boreas 9, 53–69.

Andreev, A.A., Tarasov, P.E., Romanenko, F.A., Sulerzhitsky, L.D., 1997. Younger Dryas pollen records from Sverdrup Island (Kara Sea). Quaternary International 41/42, 135–139.

Arslanov, K.A., Saveljeva, L.A., Gey, N.A., Klimanov, V.A., Chernov, S.B., Chernova, G.M., Kuzmin, G.F., Tertychnaya, T.V., Subetto, D.A., Deniskov, V.P., 1999. Chronology of vegetation and paleoclimatic stages of northwestern Russia during the Late Glacial and Holocene. Radiocarbon 41, 25–45.

Astakhov, V.I., Svendsen, J.I., Matiouchkov, A., Mangerud, J., Maslenikova, O., Tveranger, J., 1999. Marginal formations of the last Kara and Barents ice sheets in Northern Russia. Boreas 28, 23–45.

Barents Euro-Arctic Region Databank. supported by the Finnish Ministry of Trade and Industry and the Ministry of Environment. http://finnbarents.urova.fi/barentsinfo/maps/index.htm.

Berglund, B., Björck, S., Lemdahl, G., Bergsten, H., Nordberg, K., Kolstrup, E., 1994. Late Weichselian environmental change in Sweden and Denmark. Journal of Quaternary Science 9, 127–132.

Birks, H.J.B., 1968. The identification of *Betula nana* pollen. The New Phytologist 67, 309–314.

Birks, H.J.B., Line, J.M.L., 1992. The use of rarefaction analysis for estimating palynological richness from Quaternary pollen-analytical data. The Holocene 2, 1–10.

Birks, H.H., Paus, Aa., Svendsen, J.I., Alm, T., Mangerud, J., Landvik, J., 1994. Late Weichselian environmental change in Norway, including Svalbard. Journal of Quaternary Science 9, 133–145.

Björck, S., Rundgren, M., Ingolfsson, O., Funder, S., 1997. The Preboreal oscillation around the Nordic Seas: terrestrial and lacustrine responses. Journal of Quaternary Science 12, 455–465.

Björck, S., Bennike, O., Possnert, G., Wohlfart, B., Digerfeldt, G., 1998. A high-resolution ^{14}C dated sediment sequence from southwest Sweden: age comparisons between different components of the sediment. Journal of Quaternary Science 13, 85–89.

Borisova, O.K., Zelikson, E.M., 1995. Vegetation and climate of eastern Europe during the Late Glacial. In: Velichko, A.A. (Ed.), PAGES, PEP III: Climate and Environment Changes of East Europe During Holocene and Late-Middle Pleistocene, 14–19. Institute of Geography of Russian Academy of Science, Moscow.

Brown, J., Ferrians, O.J., Heginbottom, J.A., Melnikov, E.S., 1997. Circum-Arctic map of permafrost and ground-ice conditions. 1:10,000,000. US Department of the Interior, US Geological Survey, Circum-Pacific Map Series CP-45.

Dahl, S.O., Nesje, A., 1996. A new approach to calculating Holocene winter precipitation by combining glacier equilibrium-line altitudes and pine-tree limits: a case study from Hardangerjøkulen, central southern Norway. The Holocene 6, 381–398.

Davydova, N., Servant-Vildary, S., 1996. Late Pleistocene and Holocene history of the lakes in the Kola Pensinsula, Karelia and the north-western part of the east European Plain. Quaternary Science Reviews 15, 997–1012.

Dean, W.E., Forester, R.M., Bradbury, J.P., 2002. Early Holocene change in atmospheric circulation in the Northern Great Plains: an upstream view of the 8.2 ka cold event. Quaternary Science Reviews 21, 1763–1775.

Donner, J.J., Jungner, H., Vasari, Y., 1971. The hard-water effect on radiocarbon measurements of samples from Säynäjälampi, northeast Finland. Commentationes Pysico-Mathematicae 41, 307–310.

Elina, G.A., Filimonova, L.V., Klimanov, V.A., 1995. Late Glacial and Holocene paleogeography of East Fennoscandia. In: Velichko, A.A. (Ed.), Climate and Environment Changes of East Europe During Holocene and Late-Middle Pleistocene. PAGES PEP III, Moscow, pp. 20–27.

Elina, G.A., Kuznetskov, O.L., 1996. Palaeovegetation and palaeogeography of Holocene of Pribelomorskaya lowland in Karelia; prognosis for 1000 years. Aquilo Serio Botanicae 36, 9–20.

Eneroth, O., 1951. Undersökning rörande möjligheterna att i fossilt material urskilja de olika *Betula*-arternas pollen. Geologiska föreningens i Stockholm förhandlingar 73, 343–405.

Fredskild, B., 1973. Studies in the vegetational history of Greenland. Palaeobotanical investigations of some Holocene lake and bog deposits. Meddelelser om Grønland 198(4), 245pp.

Funder, S., Abrahamsen, N., 1988. Palynology in a polar desert, eastern North Greenland. Boreas 17, 195–207.
Fægri, K., Iversen, J., 1989. Textbook of pollen analysis. 4. Revised edition by Fægri, K., Kaland, P.E., Krzywinski, K. Wiley, Chichester, 314pp.
Grime, J.P., 1973. Competitive exclusion in herbaceous vegetation. Nature 242, 344–347.
Haas, J.N., Richoz, I., Tinner, W., Wick, L., 1998. Synchronous Holocene climatic oscillations recorded on the Swiss Plateau and at timberline in the Alps. The Holocene 8, 301–309.
Hahne, J., Melles, M., 1997. Late- and post-glacial vegetation and climate history of the south-western Taymyr Peninsula, central Siberia, as revealed by pollen analysis of a core from Lake Lama. Vegetation History and Archaeobotany 6, 1–8.
Hahne, J., Melles, M., 1999. Climate and vegetation history on the Taymyr Peninsula since Middle Weichselian time—Palynological evidence from lake sediments. In: Kassens, H., Bauch, H.A., Dmitrenko, I.A., Eicken, H., Hubberten, H.-W., Melles, M., Thiede, J., Timokhov, L.A. (Eds.), Land–Ocean Systems in the Siberian Arctic: Dynamics and History. Springer, Berlin, pp. 477–499.
Harrison, S.P., Yu, G., Tarasov, P.E., 1996. Late Quaternary lake-level record from northern Eurasia. Quaternary Research 45, 138–159.
Hicks, S., 1994. Present and past pollen records of Lapland forests. Review of Palaeobotany and Palynology 82, 17–35.
Hyvärinen, H., 1976. Flandrian pollen deposition rates and tree-line history in northern Fennoscandia. Boreas 5, 163–175.
Iversen, J., 1954. The Lateglacial flora of Denmark and its relation to climate and soil. Danmarks Geologiske Undersøgelse, II. Række 80, 87–119.
Jankovska, V., Vasari, Y., Elina, G.A., Kuznetsov, O.L., 1999. The Holocene palaeogeography of Paanajärvi National park, nortwestern Russia. Fennia 77, 71–82.
Johnsen, S.J., Clausen, H.B., Dansgaard, W., Fuhrer, K., Gundestrup, N., Hammer, C.U., Iversen, P., Jouzel, J., Stauffer, B., Steffensen, J.P., 1992. Irregular glacial interstadials rcorded in a new Greenland ice core. Nature 359, 311–313.
Jongman, R.H.G., Ter Braak, C.J.F., van Tongeren, O.F.R. (Eds.), 1987. Data analysis in community and landscape ecology. Pudoc, Wageningen, 299pp.
Kaakinen, A., Eronen, M., 2000. Holocene pollen stratigraphy indicating climatic and tree-line changes derived from a peat section at Ortino, in the Pechora lowland, northern Russia. The Holocene 10, 611–620.
Khain, V.E., 1985. Geology of the USSR. First Part: Old Cratons and Paleozoic Fold Belts. Gebrüder Borntraeger, Berlin, Stuttgart, 272pp.
Khotinsky, N.A., 1984. Holocene vegetation history. In: Velichko, A.A., Wright, H.E., Barnosky, C.W. (Eds.), Late Quaternary Environments of the Soviet Union. University of Minnesota Press, Minneapolis, pp. 179–200.
Khotinsky, N.A., Klimanov, V.A., 1997. Alleröd, Younger Dryas and early Holocene Palaeo-environmental stratigraphy. Quaternary International 41/42, 67–70.
Kienast, F., Siegert, C., Dereviagin, A., Mai, D.H., 2001. Climatic implications of Late Quaternary macrofossil assemblages from Taymyr Peninsula, Siberia. Global and Planetary Change 31, 265–281.
Klimanov, V.A., 1997. Late glacial climate in northern Eurasia: the last cliamatic cycle. Quaternary International 41/42, 141–152.
Klitgaard-Kristensen, D., Sejrup, H.P., Haflidason, H., Johnsen, S., Spurk, M., 1998. A regional cooling 8200 cal. yr BP cooling event in northwest Europe, induced by final stages of the Laurentide ice-sheet deglaciation? Journal of Quaternary Science 13, 165–169.
Kolstrup, E., 1979. Herbs as July temperature indicators for parts of the Pleniglacial and Lateglacial in The Netherlands. Geologie en Mijnbouw 58, 377–380.
Kondratiene, O., 1998. Periglacial sediments of the Nemunas Glaciation in North-West Lithuania. Geologija 23, 72–76.
Kremenetski, C.V., Patyk-Kara, N.G., 1997. Holocene vegetation dynamics of the southeast Kola Peninsula, Russia. The Holocene 7, 473–479.
Kremenetski, C.V., Vaschalova, T., Goriachkin, S., Cherkinsky, A., Sulerzhitsky, L., 1997. Holocene pollen stratigraphy in the western part of Kola Pensinsula, Russia. Boreas 26, 91–102.
Kremenetski, C.V., Sulerzhitsky, L.D., Hantemirov, R., 1998. Holocene history of the northern range of some trees and shrubs in Russia. Arctic and Alpine Research 30, 317–333.
Kullman, L., 1986. Demography of *Betula pubescens* ssp. *tortuosa* in contrasting habitats close to birch tree-limit in Central Sweden. Vegetatio 65, 13–20.
Kutzbach, J., Gallimore, R., Harrison, S., Behling, P., Selin, R., Laarif, F., 1998. Climate and biome simulations for the past 21,000 years. Quaternary Science Reviews 17, 473–506.
Lavrov, A.S., Potapenko, L.M., Zaitsev, A.P., Korolkova, Z.G., Meshalkin, K.A., Nikiforova, L.D., 1991. Map of the Quaternary deposits, scale 1:1000 000, sheet Q-38, 39 (Mezen). The National Geological Map of the USSR, new series. Mingeo SSSR, Leningrad.
MacDonald, G.M., 1993. Methodological falsification on the interpretation of palaeoecological records: the cause of the early Holocene birch decline in western Canada. Review of Palaeobotany and Palynology 79, 83–97.
MacDonald, G.M., Velichko, A.A., Kremenetski, C.V., Borisova, O.K., Goleva, A.A., Andreev, A.A., Cwynar, L.C., Riding, R.T., Forman, S., Edwards, T.W.D., Aravena, R., Hammarlund, D., Szeics, J.M., Gataullin, V.N., 2000a. Holocene treeline history and climate change across northern Eurasia. Quaternary Research 53, 302–311.
MacDonald, G.M., Felzer, B., Finney, B.P., Forman, S., 2000b. Holocene lake sediment record of Arctic hydrology. Journal of Paleolimnology 24, 1–14.
Mangerud, J., Svendsen, J.I., Astakhov, V.I., 1999. Age and extent of the Barents and Kara Sea ice sheets in northern Russia. Boreas 28, 46–80.
Mangerud, J., Astakhov, V.I., Murray, A., Svendsen, J.I., 2001. The chronology of a large ice-dammed lake and the Barents–Kara Ice Sheets advances, Northern Russia. Global and Planetary Change 31, 321–336.
Moe, D., 1998. Pollen production of *Alnus incana* at its south Norwegian altitudinal ecotone. Grana 37, 35–39.
Moore, P.D., Webb, J.A., Collinson, M.E., 1991. Pollen analysis. Blackwell Scientific Publications, Oxford, 216pp.
Nichols, H., 1967. The disturbance of arctic lake sediments by "bottom ice": a hazard for palynology. Arctic 20, 213–214.
NOAA NCDC Global Climate Perspective System monthly station. http://ingrid.ldgo.columbia.edu/SOURCES/.NOAA/.NCDC/.GCPS/.MONTHLY/.STATION.cuf/.
Odgaard, B.V., 1994. The Holocene vegetation history of northern West Jutland, Denmark. Opera Botanica 123, 171pp.
Odgaard, B.V., 1999. Fossil pollen as a record of past biodiversity. Journal of Biogeography 26, 7–17.
Oksanen, L., Moen, J., Helle, T., 1995. Timberline patterns in northernmost Fennoscandia. Relative importance of climate and grazing. Acta Botanica Fennica 153, 93–105.
Olsson, I., 1979. A warning against radiocarbon dating of samples containing little carbon. Boreas 8, 203–207.
Paus, Aa., 1992. Late Weichselian vegetation, climate, and floral migration in Rogaland, southwestern Norway; pollen analytical evidence from four Lateglacial basins. Dr. Thesis, University of Bergen, Norway, 87 pp.

Paus, Aa., 1995. The Late Weichselian and early Holocene history of tree birch in south Norway and the Bølling Betula time-lag in northwest Europe. Review of Palaeobotany and Palynology 85, 243–262.

Paus, Aa., 2000. Interpretative problems and sources of error related to pollen-analytical studies of the Holocene on the Timan ridge, western Pechora Basin, northern Russia. AmS-Skrifter 16. Archaeological Museum, Stavanger, Norway, 111–126.

Pennington, W., 1973. Absolute pollen frequencies in the sediment of lakes of different morphometry. In: Birks, H.J.B., West, R.G. (Eds.), Quaternary Plant Ecology. Blackwell Scientific Publications, Oxford, pp. 79–104.

Peterson, P.M., 1993. Vegetational and climatic history of the western former Soviet Union. In: Wright, H.E., Kutzbach, J.E., Webb, T., Ruddiman, W.F., Street-Perrot, F.A., Bartlein, P.J. (Eds.), Global Climate Since the Last Glacial Maximum. University of Minnesota Press, Minneapolis, pp. 169–193.

Punt, W., Blackmore, S., Clarke, G.C.S., Hoen, P.P., 1976–1995. (Eds.). The Northwest European Pollen Flora I-VII. Elsevier, Amsterdam.

Ritchie, J.C., Lichti-Federovich, S., 1967. Pollen dispersal phenomena in Arctic–Subarctic Canada. Review of Palaeobotany and Palynology 3, 255–266.

Rogers, J.C., Moseley-Thompson, E., 1995. Atlantic arctic cyclones and the mild Siberian winters of the 1980's. Geophysical Research Letters 22, 799–802.

Satkūnas, J., Kondratiene, O., 1998. Merkinė (Eemian) Interglacial deposits in the Vilnius region and the limit of the last Glaciation in southeastern Lithuania. PACT 54, 203–210.

Seppä, H., 1998. Postglacial trends in palynological richness in the northern Fennoscandian tree-line area and their ecological interpretation. The Holocene 8, 43–53.

Seppä, H., Hammarlund, D., 2000. Pollen-stratigraphical evidence of Holocene hydrological change in northern Fennoscandia supported by independent isotopic data. Journal of Paleolimnology 24, 69–79.

Serebryanny, L., Andreev, A.A., Malyasova, E., Tarasov, P., Romanenko, F., 1998. Lateglacial and early-Holocene environments of Novaya Zemlya and the Kara Sea Region of the Russian Arctic. The Holocene 8, 323–330.

Simonsen, A., 1980. Vertikale variasjoner i Holocen pollen sedimentasjon i Ulvik, Hardanger. AmS-Varia 8, 86pp.

Smilauer, P., 1992. CANODRAW 3.0. Microcomputer Power, Ithaca, New York, USA.

Snyder, J.A., MacDonald, G.M., Forman, S.L., Tarasov, G.A., Mode, W.N., 2000. Postglacial climate and vegetation history, north-central Kola Penins Russia: pollen and diatom records from Yarnyshnoe-3. Boreas 29, 261–271.

Stager, J.C., Mayewski, P.A., 1997. Abrupt early to mid-Holocene climatic transition registered at the Equator and the Poles. Science 276, 1834–1836.

Stockmarr, J., 1971. Tablets with spores in absolute pollen analysis. Pollen et Spores 13, 615–621.

Stuiver, M., Reimer, P.J., Bard, E., Beck, J.W., Burr, G.S., Hughen, K.A., Kromer, B., McCormac, G., van der Plicht, J., Spurk, M., 1998. INTCAL98 radiocarbon age calibration, 24,000-0 cal BP. Radiocarbon 40, 1041–1083.

Sutherland, D.G., 1980. Problems of radiocarbon dating deposits from newly deglaciated terrain; examples from the Scottish Lateglacial. In: Lowe, J.J., Gray, J., Robinson, J.E. (Eds.), Studies in the Lateglacial of North-West Europe. Pergamon Press, Oxford, pp. 139–149.

Svendsen, J.I., Asthakov, V.I., Bolshiyanov, D.Yu., Demidov, I., Dowdeswell, J.A., Gataullin, V., Hjort, Ch., Hubberten, H.W., Larsen, E., Mangerud, J., Melles, M., Möller, P., Saarnisto, M., Siegert, M.J., 1999. Maximum extent of the Eurasian ice sheets in the Barents and Kara Sea region during the Weichselian. Boreas 28, 234–242.

Svendsen, J.I., Alexanderson, H., Astakhov, V.I., Demidov, I., Dowdeswell, J.A., Funder, S., Gataullin, V., Henriksen, M., Hjort, Houmark-Nielsen, C., Hubberten, H.W., Ingólfsson, Ó., Jakobsson, M., Kjær, K.H., Larsen, E., Lokrantz, H., Lunkka, J.P., Lysså, A., Mangerud, J., Matiouchkov, A., Murray, A., Möller, P., Niessen, F., Nikolskaya, O., Polyak, L., Saarnisto, M., Siegert, C., Siegert, M.J., Spielhagen, R.F., Stein, R. submitted. Late Quaternary ice sheet history of Eurasia. Quaternary Science Reviews, submitted for publication.

Ter Braak, C.J.F., 1987–1992. CANOCO—a FORTRAN program for Canonical Community Ordination. Microcomputer, Ithaca, New York, USA.

Usinger, H., 1978. Pollen- und großrestanlytische Untersuchungen zur Frage des Bölling-Interstadials und der spätglazialen Baumbirken Einwanderung in Schleswig-Holstein. Schriften des Naturwissenschaftlichen Vereins fuer Schleswig-Holstein 48, 41–61.

van Leeuwaarden, W., 1982. Palynological and macropalaeobotanical studies in the development of the vegetation mosaic in eastern Noord Brabant (the Netherlands) during Lateglacial and Early Holocene times. Dr. Thesis, University of Utrecht, the Netherlands, 204pp.

Velichko, A.A., 1995. The Pleistocene termination in northern Eurasia. Quaternary International 28, 105–111.

Velichko, A.A., Andreev, A.A., Klimanov, V.A., 1997. Climate and vegetation dynamics in the tundra and forest zone during the Late Glacial and Holocene. Quaternary International 41/42, 71–96.

Walker, M.J.C., Bohncke, S.J.P., Coope, G.R., O'Connell, M., Usinger, H., Verbruggen, C., 1994. The Devensian/Weichselian Lateglacial in northwest Europe (Ireland, Britain, north Belgium, The Netherlands, northwest Germany). Journal of Quaternary Science 9, 109–118.

Webb, J.A., Moore, P.D., 1982. The late Devensian vegetational history of the Whitlaw Mosses, Southeast Scotland. New Phytologist 91, 341–398.

Wolfe, B.B., Edwards, T.W.D., Aravena, R., Forman, S.L., Warner, B.G., Velichko, A.A., MacDonald, G.M., 2000. Holocene paleohydrology and paleoclimate at treeline, North-Central Russia, inferred from oxygen isotope record in lake sediment cellulose. Quaternary Research 53, 319–329.

Zelikson, E.M., 1997. The flora and vegetation in Europe during the Allerød. Quaternary International 41/42, 97–101.